Giftet Inc.
Journal of Geolocation, Geo-information, and Geo-intelligence
Volume 2024, article ID 2024071601, 17 pages
https://doi.org/10.18610/JG3.2024.071601

Research Article

On the Landmark Hybrid Computation of the Generalized Parabolic Cylinder Function Distribution

To my Prof., John Orr, a phenomenal teacher, scholar, researcher, friend, department head, the best Ph.D. Dissertation academic advisor who I have ever known in my life.[i]

Ilir F. Progri[1]
[1]*Giftet Inc., 5 Euclid Ave. #3, Worcester, MA 01610, USA*
ORCID: 0000-0001-5197-1278
Correspondence should be addressed to Ilir Progri; iprogri@giftet.com

Received May 8, 2024; Revised May 19, 2024-June 17, 2024, Accepted July 16, 2024; Published November 1, 2024.

Editor-in-Chief/Senior Scientific Editor: Ilir F. Progri

This paper discusses the landmark hybrid computation[ii] (LHC) of the Generalized Parabolic Cylinder Function (or GPCF) distribution (or GPCFD) cumulative probability distribution function (cdf) that consists of two segments: the inner segment and the outer segment. First, the inner segment consists of the absolute values of the main variable minus a parameter are less than equal to another parameter. Second, the outer segment consists of all the values of the main variable that are outside of the inner segment. Although in the past the computation of the Efficient GPCFD (or EGPCFD) cdf existed for both of these segments; only the outer segment computation was optimized for both speed and accuracy. Third, the LHC of the GPCFD cdf is the currently fastest computation of the GPCFD cdf for the inner segment. Numerical results are derived for the first and second special cases to validate the theoretical models presented in the paper. According to the numerical results the LHC of the GPCFD cdf is several orders of magnitude more accurately and two orders of magnitude faster than any of the previous computations of the EGPCFD cdf.

Index Terms—Landmark hybrid computation, generalized parabolic cylinder function distribution, probability density function, cumulative distribution function, inner segment, outer segment, error function, complementary error function, integrals of the error function.

1 Introduction

The Landmark Hybrid Computation (LHC) of the Generalized Parabolic Cylinder Function [1]-[3] distribution (GPCFD) consists of the inner segment of the cumulative probability distribution function (cdf).

What is the definition of HC in the context of the computation (and/or HC) of various cdfs? The HC consists of the computation of cdfs whose closed form expression is only partially known via the elementary functions of other functions of the table of integrals, series, and products Gradshteyn, Ryzhik(2007, [1]). What is not known in the HC of cdfs is computed numerically via the computation of the integral routine in MATLAB.

Why is the LHC important in context of the GPCFD cdf? To understand the importance of the LHC of the GPCFD cdf we need to take a trip down the memory lane and underline the importance of every achievement that led to the LHC of the GPCFD cdf.

The study of the GPCFD pdf and cdf started in 2016 with Progri(2016 [3]). In 2016 I completely underestimated the difficulty of this problem. Even today I am surprised to see that this work, which lacks many important derivations, and a lot of other substantive investigations put me in a position that I was not able to make any kind of statements as to how the computation of the GPCFD might, should, or could look like. I had some understanding of the GPCFD pdf and I was able to prove that the GPCFD was a valid distribution, and I provided for the first time the closed form expression of the coefficient of proportionality of the GPCFD Progri(2016 [3] (56)) which ensured that the GPCFD was a valid distribution function.

From 2016 until 2021 I made almost no significant contributions in the computation of the GPCFD cdf because I worked on many other important problems somewhat related to the computation of the GPCFD cdf such as in Progri (2018, [4]) and Progri (2019, [5]). I had the impression in 2019 and 2020 that the computation of the GPCFD cdf would be computed efficiently by means of the Kampé de Fériet function or via the Srivastava's triple hypergeometric series.

In 2020 I published a very important computational research paper that immediately became a hit in Progri (2020, [6]) and in Progri (2021, [7]) that discussed a very difficult computational problem *unrelated* to the computation of the GPCFD cdf; however, then I felt that this word could be *related* to the computation of the GPCFD cdf.

By 2021 I was almost certain that the computation of the GPCFD via either the Kampé de Fériet function or via Srivastava's triple hypergeometric series was within reach as illustrated in Progri (2021, [8]-[10]). What was lacking in the computation of the GPCFD cdf? (1) the computation of the outer segment was missing; (2) the computation of the inner segment was slow; one to two orders slower than the MATLAB integral routine; (3) the accuracy cannot be guaranteed for values of a parameter greater than one. It is not to say that what was accomplished in 2021 was not significant; not at all, in 2021 the computation of the GPCDF cdf was accomplished in many different ways: via the direct MATLAB integral routine, via the linear approximation, and also via the CFE via the Kampé de Fériet function or via Srivastava's triple hypergeometric series. All the accomplishments in 2021 would not have been possible without a significant understanding of the GPCFD pdf and of the computation of the PCF.

What happened between 2022 and 2023 is that I wrote quite a bit in Progri (2022, [11]) to Progri (2023, [16]). In 2022-23 I understood that there were significant limitations from the power series expansion of the exponential models in Progri (2022, [11]) and of the Hermite Polynomial expansion of the exponential model when a negative exponent is the square of the main variable in Progri (2023, [15]). What was significant about these works is that they showed that the main reason why the solution in Progri (2021, [8]-[10]) was limited in both speed and accuracy was due to the limitations of the models that I employed. In 2022-23 I attempted to fix most of the shortcomings associated with the computation of the tail distribution in Progri (2022, [13]), Progri (2023, [16]).

Having tried basically almost anything, I came to the realization that currently the most efficient way to compute the GPCFD cdf is via the LHC method.

Looking back at the amount of work that was produced from Progri(2016, [3]) to Progri (2023, [16]) then the natural question is why did it take me so long to produce the HC method? Th LHC method should have been the first method to have been used or at least the LHC method should have been employed by 2021 at the very least. Moreover, I do not believe that the HC method will be the last computational method utilized to efficiently compute the GPCFD cdf; however, based on the numerical results shown in this paper the LHC method is the most efficient method to date.

This paper is organized as follows: in Sect. 2 the computation of the GPCFD pdf is presented. The LHC of the GPCFD is discussed in Sect. 3. Section 4 contains numerical results; Conclusion is provided in Sect. 5, Acknowledgment in Sect. 6, along with a list of references in Sect. 7. The derivations or deduction of integral (44) and (47) are presented in Appen. A and B respectively; and the details and ingredients of integrals (58), (61) and (68), (71) are shown in Appen. C and D. respectively.

This concludes with the introduction Sect. of the paper. Next, we start with the computation of the GPCFD pdf.

2 The Computation of the GPCFD PDF

In this section the computation of the GPCFD pdf is performed. The GPCFD contains two main computations: first, the GPCFD pdf is discussed in Sect. 2.1; and second, the CGPCFD pdf is discussed in Sect. 2.2.

2.1 The GPCFD PDF

In writing the GPCFD pdf we will use two different segments for its representation. First, starting with the original definition of the GPCFD pdf, $f(x)$, (see Progri (2016, [3] (1)-(10)) we have,

$$f(x)=\frac{d_0(x)\sum_{r=0}^{N-1}p_-!a^pH_r(N)\left[b_0(x)D_{-p}[c_0(x)]+b_1(x)D_{-p}[c_1(x)]\right]}{C} \quad (1)$$

where $0<a,b,c<\infty$ and $N\geq 1$ positive integer

$p=N-r; p>0$, positive integer (2)

$p_-=p-1$ non-negative integer (3)

$$D_{-p}(z_i\equiv z)=2^{\frac{p}{2}}e^{-\frac{z^2}{4}}U\left(-\frac{p}{2},\frac{1}{2},\frac{z^2}{2}\right), \text{PCF} \quad (4)$$

$b_i(x), i=\{0,1\}$ is given by (see Progri(2016, [3] (3)), $H_r(N)$ is the Hermite polynomials (see Gradshteyn, Ryzhik(2007, [1] pg. 996 8.95));

where z_i is defined as being equal to $c_i(x)$ (see Progri(2016, [3] (4))

$$z_i=c_i(x); i=\{0,1\}$$
$$=a\left[\frac{1}{c^2}-(-1)^ia_0(x)\right] \quad (5)$$

In Appen. A we discuss as to why $0<a,b,c<\infty$ in contrast to previous publications Progri(2016, [3]), Progri(2021, [8]-[10]), Progri(2023, [14], [16]).

The normally distributed component $d_0(x)$ corresponding to *the inner segment* is given by (see Progri(2016, [3] (5)), Progri(2021, [8] (47)) and in other places)

$$d_0(x)=e^{-a_0(x)(x-b)}=e^{-\frac{(x-b)^2}{2a^2}}=e^{-2a^2a_0^2(x)} \quad (6)$$

However, the normally distributed components $q_i(x)$, $i=\{0,1\}$ corresponding to *the outer segment* Progri(2021, [8] (48), (49)) is written as

$$q_i(x)=e^{-\frac{1}{2}g_i^2(x)}=e^{-\frac{1}{2}\left[\frac{\sqrt{3}(x-b)}{2a}+\frac{(-1)^ia}{\sqrt{3}c^2}\right]^2}; i=\{0,1\} \quad (7)$$

Using the above definition (5) we can write the Tricomi confluent hypergeometric function (TCHF), $U(a,b,z)$, and a Tricomi like confluent hypergeometric function (TLCHF), $V_i(-p,x)$, as follows

$$U\left(\frac{p}{2},\frac{1}{2},\frac{z_i^2}{2}\right)=\frac{\sqrt{\pi}M\left[\frac{p}{2},\frac{1}{2}\middle|\frac{z_i^2}{2}\right]}{\Gamma\left(\frac{1+p}{2}\right)}-\frac{\sqrt{2\pi}z_iM\left[\frac{1+p}{2},\frac{3}{2}\middle|\frac{z_i^2}{2}\right]}{\Gamma\left(\frac{p}{2}\right)} \quad (8)$$

$$V_i(-p,x)=\frac{M\left[\frac{1-p}{2},\frac{1}{2}\middle|-\frac{z_i^2}{2}\right]}{\Gamma\left(\frac{1+p}{2}\right)}-\frac{\sqrt{2}z_iM\left[\frac{2-p}{2},\frac{3}{2}\middle|-\frac{z_i^2}{2}\right]}{\Gamma\left(\frac{p}{2}\right)} \quad (9)$$

The normalization coefficient, C, was computed in (see Progri (2016, [2] (56)).

Second, assuming that $x_0\gg 1$, then we can write the GPCFD pdf invoking Progri (2021, [8] (31) and (51)) as follows,

$$f(x)=\begin{cases}\dfrac{d_0(x)\sum_{r=0}^{N-1}\frac{p_-!\left[U\left(\frac{p}{2},\frac{1}{2},\frac{z_0^2}{2}\right)+U\left(\frac{p}{2},\frac{1}{2},\frac{z_1^2}{2}\right)\right]}{2^{0.5p}H_r(N)^{-1}a^{-p}}}{C}; & |x-b|<x_0\\ \dfrac{\sum_{r=0}^{N-1}\frac{p_-![q_0(x)V_0(-p,x)+q_1(x)V_1(-p,x)]}{2^{0.5p}H_r(N)^{-1}a^{-p}}}{\pi^{-0.5}e^{\frac{-2a^2}{3c^4}}C}; & |x-b|\geq x_0\end{cases} \quad (10)$$

On in a more compact notation, $f(x)$, can be expressed as composed of two main segments, the inner segment, $f_{in}(x)$, and the other segment, $f_{ou}(x)$, as given below

$$f(x)=\begin{cases}f_{in}(x); & |x-b\equiv x_{-b}|\leq x_0\\ f_{ou}(x); & |x_{-b}|\geq x_0\end{cases} \quad (11)$$

In Progri(2021, [8]) it was already shown that the $f_{in}(x)\equiv f_{ou}(x)$ for $-\infty<x<\infty$; however, it is more convenient to use the above notations for the reasons explained later in the paper.

This concludes the discussion on the GPCFD pdf. Next, we discuss a couple of special cases.

2.1.1 First Special Case of the GPCFD PDF

The first special case occurs when

$N=1\Rightarrow p=1; r=0$ (12)

Next, substituting (12) into (10) or (11) yields,

$$f(x)=\left|\begin{array}{ll}\dfrac{d_0(x)\dfrac{p-!\left[U\left(\frac{p=1}{2},\frac{1}{2},\frac{z_0^2}{2}\right)+U\left(\frac{p}{2},\frac{1}{2},\frac{z_1^2}{2}\right)\right]}{2^{0.5p}H_0(N)^{-1}a^{-p}}}{C}; & |x-b|<x_0\\ \dfrac{q_0(x)V_0(-1,x)+q_1(x)V_1(-1,x)}{\pi^{-0.5}2^{0.5}a^{-1}e^{\frac{-2a^2}{3c^4}}C}; & |x-b|\geq x_0\end{array}\right.$$

$$=\left|\begin{array}{ll}\dfrac{d_0(x)\left[U\left(\frac{1}{2},\frac{1}{2},\frac{z_0^2}{2}\right)+U\left(\frac{1}{2},\frac{1}{2},\frac{z_1^2}{2}\right)\right]}{a^{-1}2^{0.5}C}; & |x-b|<x_0\\ \dfrac{q_0(x)V_0(-1,x)+q_1(x)V_1(-1,x)}{\pi^{-0.5}2^{0.5}a^{-1}e^{\frac{-2a^2}{3c^4}}C}; & |x-b|\geq x_0\end{array}\right. \tag{13}$$

First, substituting (12) into (8) and (9) produces,

$$U\left(\frac{1}{2},\frac{1}{2},\frac{z_i^2}{2}\right)=\frac{\sqrt{\pi}M\left[\frac{1}{2},\frac{1}{2}\middle|\frac{z_i^2}{2}\right]}{\Gamma(1)}-\frac{\sqrt{2\pi}z_iM\left[1,\frac{3}{2}\middle|\frac{z_i^2}{2}\right]}{\Gamma\left(\frac{1}{2}\right)}$$

$$=\sqrt{\pi}e^{\frac{z_i^2}{2}}-\sqrt{2}z_ie^{\frac{z_i^2}{2}}M\left[\frac{1}{2},\frac{3}{2}\middle|-\frac{z_i^2}{2}\right]\ (\text{KFT}^{\text{iii}})$$

$$=\sqrt{\pi}e^{\frac{z_i^2}{2}}-e^{\frac{z_i^2}{2}}\sqrt{\pi}\Phi\left(\frac{z_i}{\sqrt{2}}\right)$$

$$=\sqrt{\pi}e^{\frac{z_i^2}{2}}\left[1-\Phi\left(\frac{z_i}{\sqrt{2}}\right)\equiv\Phi_c\left(\frac{z_i}{\sqrt{2}}\right)\right]$$

$$=\sqrt{\pi}e^{\frac{z_i^2}{2}}V_i(-1,x) \tag{14}$$

$$V_i(-1,x)=1-\frac{\sqrt{2}z_iM\left[\frac{1}{2},\frac{3}{2}\middle|-\frac{z_i^2}{2}\right]}{\sqrt{\pi}}$$

$$=1-\Phi\left(\frac{z_i}{\sqrt{2}}\right)\equiv\Phi_c\left(\frac{z_i}{\sqrt{2}}\right) \tag{15}$$

Next, substituting (14) and (15) into (13) yields

$$f(x)=\left|\begin{array}{ll}\dfrac{d_0(x)\left[e^{\frac{z_0^2}{2}}V_0(-1,x)+e^{\frac{z_1^2}{2}}V_1(-1,x)\right]}{\pi^{-0.5}2^{0.5}a^{-1}C}; & |x-b|<x_0\\ \dfrac{q_0(x)\Phi_c\left(\frac{z_0}{\sqrt{2}}\right)+q_1(x)\Phi_c\left(\frac{z_1}{\sqrt{2}}\right)}{\pi^{-0.5}2^{0.5}a^{-1}e^{\frac{-2a^2}{3c^4}}C}; & |x-b|\geq x_0\end{array}\right. \tag{16}$$

The normalization coefficient can be computed from Progri(2016, [3] (56) pg. 77)

$$C=\frac{4\sqrt{\pi}e^{\frac{a^2}{3c^4}}\frac{2a}{\sqrt{3}}aH_0(1)0!D_{-1}\left(\frac{2a}{\sqrt{3c^2}}\right)}{\sqrt{2}}$$

$$=\frac{4\sqrt{2}a^2\sqrt{\pi}e^{\frac{a^2}{3c^4}}e^{\frac{a^2}{3c^4}}\sqrt{\frac{\pi}{2}}\left[1-\Phi\left(\frac{y}{\sqrt{2}}\right)\right]}{\sqrt{3}}$$

$$=\frac{4a^2\pi e^{\frac{2a^2}{3c^4}}\Phi_c\left(\frac{\sqrt{2}a}{\sqrt{3c^2}}\right)}{\sqrt{3}} \tag{17}$$

What we see in (16) is that for $1\ll x_0<\infty$, *the inner segment* of $f(x)$ is a product of two functions that does not lead to any singularities. *The outer segment* is already discussed in Progri (2021, [8]).

Next, recognizing that the product of $d_0(x)$ with $e^{z_i^2/2}$ equal to the product of $q_i(x)$ with a constant term, $e^{2a^2/3c^4}$

$$d_0(x)e^{\frac{z_i^2}{2}}=e^{-\frac{1}{2}g_i^2(x)}e^{\frac{2a^2}{3c^4}}=q_i(x)e^{\frac{2a^2}{3c^4}} \tag{18}$$

Substituting (18) into (16) we obtain,

$$f(x)=\left|\begin{array}{ll}\dfrac{q_0(x)\Phi_c\left(\frac{z_0}{\sqrt{2}}\right)+q_1(x)\Phi_c\left(\frac{z_1}{\sqrt{2}}\right)}{\pi^{-0.5}2^{0.5}a^{-1}e^{\frac{-2a^2}{3c^4}}C}; & |x-b|<x_0\\ \dfrac{q_0(x)\Phi_c\left(\frac{z_0}{\sqrt{2}}\right)+q_1(x)\Phi_c\left(\frac{z_1}{\sqrt{2}}\right)}{\pi^{-0.5}2^{0.5}a^{-1}e^{\frac{-2a^2}{3c^4}}C}; & |x-b|\geq x_0\end{array}\right. \tag{19}$$

We can then write the GPCFD pdf as follows,

$$f(x)=\frac{q_0(x)\Phi_c\left(\frac{z_0}{\sqrt{2}}\right)+q_1(x)\Phi_c\left(\frac{z_1}{\sqrt{2}}\right)}{\pi^{-0.5}2^{0.5}a^{-1}e^{\frac{-2a^2}{3c^4}}C},\ -\infty<x<\infty \tag{20}$$

Equation (20) is identical to Progri(2021, [10] (2) pg. 47).

We see in this first example that we have more options for computing the GPCFD pdf and then the corresponding cdf: we can compute the GPCFD pdf inner segment and then the outer segment (16) or the entire function as in (18) or (19).

This concludes the discussion of the first special case of the GPCFD pdf.

2.1.2 Second Special Case of the GPCFD PDF

The second special case occurs when the following is true Progri(2021, [8], [10])

$$N=2\Rightarrow r=\{0,1\};\ p=\{2,1\} \tag{21}$$

The GPCFD pdf corresponding to (21) is given by the shorthand notation as below,

$$f(x)=\left|\begin{array}{ll}f_{in}(x); & |x_{-b}|<x_0\\ f_{ou}(x); & |x_{-b}|\geq x_0\end{array}\right. \tag{22}$$

where

$$f_{in}(x)=\frac{\dfrac{p-!\left[U\left(\frac{p=2}{2},\frac{1}{2},\frac{z_0^2}{2}\right)+U\left(\frac{p}{2},\frac{1}{2},\frac{z_1^2}{2}\right)\right]}{2^{0.5p}H_0(2)^{-1}a^{-p}}+\dfrac{p-!\left[U\left(\frac{p=1}{2},\frac{1}{2},\frac{z_0^2}{2}\right)+U\left(\frac{p}{2},\frac{1}{2},\frac{z_1^2}{2}\right)\right]}{2^{0.5p}H_1(2)^{-1}a^{-p}}}{d_0^{-1}(x)C}$$

$$=\frac{\dfrac{U\left(1,\frac{1}{2},\frac{z_0^2}{2}\right)+U\left(1,\frac{1}{2},\frac{z_1^2}{2}\right)}{2a^{-2}}+\dfrac{U\left(\frac{1}{2},\frac{1}{2},\frac{z_0^2}{2}\right)+U\left(\frac{1}{2},\frac{1}{2},\frac{z_1^2}{2}\right)}{2^{0.5}2^{-2}a^{-1}}}{d_0^{-1}(x)C} \tag{23}$$

$$f_{ou}(x)=\frac{\dfrac{q_0(x)V_0(-2,x)+q_1(x)V_1(-2,x)}{2a^{-2}}+\dfrac{q_0(x)V_0(-1,x)+q_1(x)V_1(-1,x)}{2^{0.5}2^{-2}a^{-1}}}{\pi^{-0.5}e^{\frac{-2a^2}{3c^4}}C} \tag{24}$$

where the normalization coefficient can be computed from Progri(2016, [3] (56) pg. 77)

$$C=\frac{4\sqrt{\pi}e^{\frac{a^2}{3c^4}}\left(\frac{2a}{\sqrt{3}}\right)^2a\sum_{k=0}^{1}H_k(2)n!\left(\frac{\sqrt{3}}{2a}\right)^kD_{k-N}\left(\frac{2a}{\sqrt{3c^2}}\right)}{\sqrt{2}}$$

$$=\frac{4\sqrt{\pi}e^{\frac{a^2}{3c^4}}\left(\frac{2a}{\sqrt{3}}\right)^2a\left[H_0(2)D_{-2}\left(\frac{2a}{\sqrt{3c^2}}\right)+H_1(2)\frac{\sqrt{3}}{2a}D_{-1}\left(\frac{2a}{\sqrt{3c^2}}\right)\right]}{\sqrt{2}}$$

$$= \frac{4^2\sqrt{\pi}a^3 e^{\frac{2a^2}{3c^4}}\sqrt{\frac{\pi}{2}}\left[\sqrt{\frac{2}{\pi}}e^{-\frac{2a^2}{3c^4}} - \frac{2a}{\sqrt{3}c^2}\Phi_c\left(\frac{\sqrt{2}a}{\sqrt{3}c^2}\right) + 2\frac{\sqrt{3}}{a}\Phi_c\left(\frac{\sqrt{2}a}{\sqrt{3}c^2}\right)\right]}{3\sqrt{2}}$$

$$= \frac{2^3\sqrt{2\pi}a^3\left[1 + e^{\frac{2a^2}{3c^4}}\sqrt{2\pi}\left(\frac{\sqrt{3}}{a} - \frac{a}{\sqrt{3}c^2}\right)\Phi_c\left(\frac{\sqrt{2}a}{\sqrt{3}c^2}\right)\right]}{3} \tag{25}$$

Where From (see Gradshteyn, Ryzhik (2007, [1] pg. 1030 9.254 2.) we have

$$D_{-2}(y) = e^{\frac{y^2}{4}}\sqrt{\frac{\pi}{2}}\left[\sqrt{\frac{2}{\pi}}e^{-\frac{y^2}{2}} - y\Phi_c\left(\frac{y}{\sqrt{2}}\right)\right] \tag{26}$$

The unknows in (23) TCHF $U\left[1, \frac{1}{2}, \frac{z_i^2}{2}\right]$ are given by

$$U\left[1, \frac{1}{2}, \frac{z_i^2}{2}\right] = \frac{\sqrt{\pi}M\left[1, \frac{1}{2}\middle|\frac{z_i^2}{2}\right]}{\Gamma\left(\frac{3}{2}\right)} - \frac{\sqrt{2\pi}z_i M\left[\frac{3}{2}, \frac{3}{2}\middle|\frac{z_i^2}{2}\right]}{\Gamma(1)}$$

$$= \frac{\sqrt{\pi}M\left[1, \frac{1}{2}\middle|\frac{z_i^2}{2}\right]}{\Gamma\left(\frac{3}{2}\right)} - \frac{\sqrt{2\pi}z_i e^{\frac{z_i^2}{2}}}{\Gamma(1)} \tag{27}$$

The CHF $M\left[1, \frac{1}{2}\middle|\frac{z_i^2}{2}\right]$ can be computed from,

$$M\left[1, \frac{1}{2}\middle|z\right] = \sum_{n=0}^{\infty}\frac{(1)_n}{\left(\frac{1}{2}\right)_n}\frac{z^n}{n!} = 1 + \sum_{k+1=1}^{\infty}\frac{(1)_{k+1}}{\left(\frac{1}{2}\right)_{k+1}}\frac{z^{k+1}}{(k+1)!}$$

$$= 1 + z\sum_{k=0}^{\infty}\frac{(1)_{k+1}}{\left(\frac{1}{2}\right)_{k+1}}\frac{z^k}{(k+1)!}$$

$$= 1 + 2z\sum_{k=0}^{\infty}\frac{(2)_k(1)_k}{\left(\frac{3}{2}\right)_k}\frac{z^k}{(k+1)!k!}$$

$$= 1 + 2z\sum_{k=0}^{\infty}\frac{(1)_k}{\left(\frac{3}{2}\right)_k}\frac{z^k}{k!}$$

$$= 1 + 2zM\left[1, \frac{3}{2}\middle|z\right]$$

$$= 1 + 2z\frac{e^z\sqrt{\pi}\Phi(\sqrt{z})}{2\sqrt{z}}$$

$$= 1 + \sqrt{\pi}\sqrt{z}e^z\Phi(\sqrt{z}) \tag{28}$$

In the above computation we made use of the following simplifications that come from the use of the Pochhammer symbol (or the rising factorial [1]) and Gamma function [1],

$$(1)_{k+1} = \frac{\Gamma(2+k)}{\Gamma(1)} = (2)_k\Gamma(2) \tag{29}$$

$$\left(\frac{1}{2}\right)_{k+1} = \frac{\Gamma\left(\frac{3}{2}+k\right)}{\Gamma\left(\frac{1}{2}\right)} = \frac{\left(\frac{3}{2}\right)_k\Gamma\left(\frac{3}{2}\right)}{\Gamma\left(\frac{1}{2}\right)} = \frac{\left(\frac{3}{2}\right)_k\frac{1}{2}\Gamma\left(\frac{1}{2}\right)}{\Gamma\left(\frac{1}{2}\right)} = \frac{\left(\frac{3}{2}\right)_k}{2} \tag{30}$$

Substituting (28) into (27) yields and original expression of the TCHF, $U\left[1, \frac{1}{2}, \frac{z_i^2}{2}\right]$,

$$U\left[1, \frac{1}{2}, \frac{z_i^2}{2}\right] = 2M\left[1, \frac{1}{2}\middle|\frac{z_i^2}{2}\right] - \sqrt{2\pi}z_i e^{\frac{z_i^2}{2}}$$

$$= 2\left[1 + \sqrt{\pi}\frac{z_i}{\sqrt{2}}e^{\frac{z_i^2}{2}}\Phi\left(\frac{z_i}{\sqrt{2}}\right)\right] - \sqrt{2\pi}z_i e^{\frac{z_i^2}{2}}$$

$$= 2 - \sqrt{2\pi}z_i e^{\frac{z_i^2}{2}}\Phi_c\left(\frac{z_i}{\sqrt{2}}\right)$$

$$= \sqrt{\pi}e^{\frac{z_i^2}{2}}2\left[e^{-\frac{z_i^2}{2}}\frac{1}{\sqrt{\pi}} - \frac{z_i}{\sqrt{2}}\Phi_c\left(\frac{z_i}{\sqrt{2}}\right)\right]$$

$$= 2^{-1}e^{\frac{z_i^2}{4}}D_{-2}(z_i)$$

$$= \sqrt{\pi}e^{\frac{z_i^2}{2}}V_i(-2, x) \tag{31}$$

The CFE for the TLCHF is given by,

$$V_i(-2, x) = \frac{M\left(\frac{-1}{2}, \frac{1}{2}\middle| -\frac{z_i^2}{2}\right)}{\Gamma\left(\frac{3}{2}\right)} - \frac{\sqrt{2\pi}z_i}{\Gamma\left(\frac{1}{2}\right)}$$

$$= \frac{M\left(\frac{-1}{2}, \frac{1}{2}\middle| -\frac{z_i^2}{2}\right)}{\frac{1}{2}\Gamma\left(\frac{1}{2}\right)} - \frac{\sqrt{2\pi}z_i}{\Gamma\left(\frac{1}{2}\right)}$$

$$= \frac{e^{-\frac{z_i^2}{2}} + \sqrt{\pi}\frac{z_i}{\sqrt{2}}\Phi\left(\frac{z_i}{\sqrt{2}}\right)}{\frac{1}{2}\Gamma\left(\frac{1}{2}\right)} - \frac{\sqrt{2\pi}z_i}{\Gamma\left(\frac{1}{2}\right)} \text{ (Progri(2021, [9] (76)))}$$

$$= \frac{2e^{-\frac{z_i^2}{2}} - \sqrt{2\pi}z_i\left[1 - \Phi\left(\frac{z_i}{\sqrt{2}}\right)\right]}{\Gamma\left(\frac{1}{2}\right)}; \text{ (Progri(2021,[10] (5)))}$$

$$= \frac{2e^{-\frac{z_i^2}{2}} - \sqrt{2\pi}z_i\Phi_c\left(\frac{z_i}{\sqrt{2}}\right)}{\Gamma\left(\frac{1}{2}\right)};$$

$$= 2\left[e^{-\frac{z_i^2}{2}}\frac{1}{\sqrt{\pi}} - \frac{z_i}{\sqrt{2}}\Phi_c\left(\frac{z_i}{\sqrt{2}}\right)\right] \tag{32}$$

Next, substituting (31) into the partial numerator of (23) yields,

$$\frac{U\left(1, \frac{1}{2}, \frac{z_0^2}{2}\right) + U\left(1, \frac{1}{2}, \frac{z_1^2}{2}\right)}{2a^{-2}} = \frac{e^{\frac{z_0^2}{2}}V_0(-2, x) + e^{\frac{z_1^2}{2}}V_1(-2, x)}{2\pi^{-0.5}a^{-2}} \tag{33}$$

Next, substituting (33) into the inner segment of (23) we have

$$f_{in}(x) = \frac{\frac{U\left(1, \frac{1}{2}, \frac{z_0^2}{2}\right) + U\left(1, \frac{1}{2}, \frac{z_1^2}{2}\right)}{2a^{-2}} + \frac{U\left(\frac{1}{2}, \frac{1}{2}, \frac{z_0^2}{2}\right) + U\left(\frac{1}{2}, \frac{1}{2}, \frac{z_1^2}{2}\right)}{2^{0.5}2^{-2}a^{-1}}}{d_0^{-1}(x)C}$$

$$
= \frac{\dfrac{\dfrac{\sqrt{\pi}M\left[1,\frac{1}{2}\middle|\frac{z_0^2}{2}\right]}{\Gamma\left(\frac{3}{2}\right)}-\dfrac{\sqrt{2\pi}z_0M\left[\frac{3}{2},\frac{3}{2}\middle|\frac{z_0^2}{2}\right]}{\Gamma(1)}+\dfrac{\sqrt{\pi}M\left[1,\frac{1}{2}\middle|\frac{z_1^2}{2}\right]}{\Gamma\left(\frac{3}{2}\right)}-\dfrac{\sqrt{2\pi}z_1M\left[\frac{3}{2},\frac{3}{2}\middle|\frac{z_1^2}{2}\right]}{\Gamma(1)}}{2a^{-2}}+\dfrac{\dfrac{\sqrt{\pi}M\left[\frac{1}{2},\frac{1}{2}\middle|\frac{z_0^2}{2}\right]}{\Gamma(1)}-\dfrac{\sqrt{2\pi}z_0M\left[1,\frac{3}{2}\middle|\frac{z_0^2}{2}\right]}{\Gamma\left(\frac{1}{2}\right)}+\dfrac{\sqrt{\pi}M\left[\frac{1}{2},\frac{1}{2}\middle|\frac{z_1^2}{2}\right]}{\Gamma(1)}-\dfrac{\sqrt{2\pi}z_1M\left[1,\frac{3}{2}\middle|\frac{z_1^2}{2}\right]}{\Gamma\left(\frac{1}{2}\right)}}{2^{0.5}2^{-2}a^{-1}}}{d_0^{-1}(x)C}
$$

$$
= \frac{\dfrac{2M\left[1,\frac{1}{2}\middle|\frac{z_0^2}{2}\right]-\sqrt{2\pi}z_0e^{\frac{z_0^2}{2}}+2M\left[1,\frac{1}{2}\middle|\frac{z_1^2}{2}\right]-\sqrt{2\pi}z_1e^{\frac{z_1^2}{2}}}{2a^{-2}}+\dfrac{\sqrt{\pi}e^{\frac{z_0^2}{2}}-\sqrt{\pi}z_0M\left[1,\frac{3}{2}\middle|\frac{z_0^2}{2}\right]+\sqrt{\pi}e^{\frac{z_1^2}{2}}-\sqrt{2}z_1M\left[1,\frac{3}{2}\middle|\frac{z_1^2}{2}\right]}{2^{0.5}2^{-2}a^{-1}}}{d_0^{-1}(x)C}
$$

$$
= \frac{\dfrac{2M\left[1,\frac{1}{2}\middle|\frac{z_0^2}{2}\right]-\sqrt{2\pi}z_0e^{\frac{z_0^2}{2}}+2M\left[1,\frac{1}{2}\middle|\frac{z_1^2}{2}\right]-\sqrt{2\pi}z_1e^{\frac{z_1^2}{2}}}{2a^{-2}}+\dfrac{\sqrt{\pi}e^{\frac{z_0^2}{2}}-e^{\frac{z_0^2}{2}}\sqrt{\pi}\Phi\left(\frac{z_0}{\sqrt{2}}\right)+\sqrt{\pi}e^{\frac{z_1^2}{2}}-e^{\frac{z_1^2}{2}}\sqrt{\pi}\Phi\left(\frac{z_1}{\sqrt{2}}\right)}{2^{0.5}2^{-2}a^{-1}}}{d_0^{-1}(x)C}
$$

$$
= \frac{\dfrac{\sqrt{\pi}e^{\frac{z_0^2}{2}}\left[e^{-\frac{z_0^2}{2}}\frac{1}{\sqrt{\pi}}-\frac{z_0}{\sqrt{2}}\Phi_c\left(\frac{z_0}{\sqrt{2}}\right)\right]+\sqrt{\pi}e^{\frac{z_1^2}{2}}\left[e^{-\frac{z_1^2}{2}}\frac{1}{\sqrt{\pi}}-\frac{z_1}{\sqrt{2}}\Phi_c\left(\frac{z_0}{\sqrt{2}}\right)\right]}{a^{-2}}+\dfrac{\sqrt{\pi}e^{\frac{z_0^2}{2}}\Phi_c\left(\frac{z_0}{\sqrt{2}}\right)+\sqrt{\pi}e^{\frac{z_1^2}{2}}\Phi_c\left(\frac{z_1}{\sqrt{2}}\right)}{2^{0.5}2^{-2}a^{-1}}}{d_0^{-1}(x)C}
$$

$$
= \frac{\sqrt{\pi}\dfrac{\sum_{i=0}^{1}e^{\frac{z_i^2}{2}}\dfrac{\left[2e^{-\frac{z_i^2}{2}}-\sqrt{2\pi}z_i\Phi_c\left(\frac{z_i}{\sqrt{2}}\right)\right]}{\sqrt{\pi}}}{2a^{-2}}+\dfrac{4a\sqrt{\pi}\sum_{i=0}^{1}e^{\frac{z_i^2}{2}}\Phi_c\left(\frac{z_i}{\sqrt{2}}\right)}{2^{0.5}}}{d_0^{-1}(x)C}
$$

$$
= \frac{a^2\sqrt{\pi}\sum_{i=0}^{1}e^{\frac{z_i^2}{2}}\left[\frac{1}{\sqrt{\pi}}e^{-\frac{z_i^2}{2}}-\frac{1}{\sqrt{2}}z_i\Phi_c\left(\frac{z_i}{\sqrt{2}}\right)+\frac{4\Phi_c\left(\frac{z_i}{\sqrt{2}}\right)}{a\sqrt{2}}\right]}{d_0^{-1}(x)C}
$$

$$
= \frac{a\sum_{i=0}^{1}e^{\frac{z_i^2}{2}}\left[e^{-\frac{z_i^2}{2}}\frac{1}{\sqrt{\pi}}+\frac{\Phi_c\left(\frac{z_i}{\sqrt{2}}\right)}{\sqrt{2}}\left(\frac{4}{a}-z_i\right)\right]}{a^{-1}\pi^{-0.5}d_0^{-1}(x)C}
$$

$$
= \frac{a\sum_{i=0}^{1}q_i(x)\left[e^{-\frac{z_i^2}{2}}\frac{1}{\sqrt{\pi}}+\frac{\Phi_c\left(\frac{z_i}{\sqrt{2}}\right)}{\sqrt{2}}\left(\frac{4}{a}-z_i\right)\right]}{a^{-1}\pi^{-0.5}e^{\frac{-2a^2}{3c^4}}C} \tag{34}
$$

Next, substituting (32) into the outer segment of (24) yields,

$$
f_{ou}(x) = \frac{\dfrac{q_0(x)V_0(-2,x)+q_1(x)V_1(-2,x)}{2a^{-2}}+\dfrac{q_0(x)V_0(-1,x)+q_1(x)V_1(-1,x)}{2^{0.5}2^{-2}a^{-1}}}{\pi^{-0.5}e^{\frac{-2a^2}{3c^4}}C}
$$

$$
= \frac{\dfrac{e^{\frac{z_0^2}{2}}V_0(-2,x)+e^{\frac{z_1^2}{2}}V_1(-2,x)}{2a^{-2}}+\dfrac{e^{\frac{z_0^2}{2}}V_0(-1,x)+e^{\frac{z_1^2}{2}}V_1(-1,x)}{2^{0.5}2^{-2}a^{-1}}}{d_0^{-1}(x)\pi^{-0.5}C}
$$

$$
= \frac{a\sum_{i=0}^{1}e^{\frac{z_i^2}{2}}\left[e^{-\frac{z_i^2}{2}}\frac{1}{\sqrt{\pi}}+\frac{\Phi_c\left(\frac{z_i}{\sqrt{2}}\right)}{\sqrt{2}}\left(\frac{4}{a}-z_i\right)\right]}{a^{-1}\pi^{-0.5}d_0^{-1}(x)C}
$$

$$
= \frac{a\sum_{i=0}^{1}q_i(x)\left[e^{-\frac{z_i^2}{2}}\frac{1}{\sqrt{\pi}}+\frac{\Phi_c\left(\frac{z_i}{\sqrt{2}}\right)}{\sqrt{2}}\left(\frac{4}{a}-z_i\right)\right]}{a^{-1}\pi^{-0.5}e^{\frac{-2a^2}{3c^4}}C} \tag{35}
$$

Equations (34) and (35) are identical to Progri(2021, [10] (6) pg. 48). From this second example we have more options for computing the GPCFD pdf and then the corresponding cdf: we can compute the GPCFD pdf inner segment as in (23) and then the outer segment (24) or the entire function as in (34) or (35). This concludes the discussion of the second special case of the EGPCFD pdf.

2.2 *The CGPCFD pdf*

The CGPCFD pdf is made of two segments. On the first segment we can employ the inner segment, $f_{in}(x)$, from (10) and the other segment, $f_{ou}(x)$, from Progri(2023, [16] (17)), which produces exactly the same pdf as follows,

$$
f(x) = \frac{e^{-2a^2[a_0(x)]^2}W_{-p}(x)}{C} \tag{36}
$$

where we have a new definition for the $W_{-p}(x)$ for inner segment

$$
W_{-p}(x) = \begin{vmatrix} \sum_{r=0}^{N-1}\dfrac{p_-!\left[U\left(\frac{p}{2},\frac{1}{2},\frac{z_0^2}{2}\right)+U\left(\frac{p}{2},\frac{1}{2},\frac{z_1^2}{2}\right)\right]}{2^{0.5p}H_r(N)^{-1}a^{-p}}; & |x-b| < x_0 \\ \sum_{r=0}^{N-1}\dfrac{p_-!\{U_{-p}[c_0(x)]+U_{-p}[c_1(x)]\}}{H_r(N)^{-1}a^{-p}}; & |x-b| \geq x_0 \end{vmatrix} \tag{37}
$$

The rest of the calculations are identical to either Sect. 2.1.1 or 2.1.2 or Progri(2023, [16] Sect. 2.3). This concludes the brief discussion on the CGPCFD pdf.

3 The LHC of the GPCFD CDF

In Progri (2021, [10] (55)) I made a statement saying: "Integral (55) is extremely difficult … I will provide that solution is another journal paper."

First, the cdf, is defined as the integral of the pdf function, $f(t)$, from minus infinity to x: composed of two main segments, the inner segment, $F_{in}(x)$, for the absolute values of x less than or equal to x_0, and of the outer segment, $F_{ou}(x)$, for absolute values of x greater than or equal to x_0 as follows,

$$
F(x) = \int_{-\infty}^{x} f(t)dt
$$

$$
= \begin{vmatrix} F_{in}(x), & |x| \leq x_0 \\ F_{ou}(x), & |x| > x_0 \end{vmatrix}, x_0 \gg (b,0) \tag{38}
$$

The *inner* cdf segment $F_{in}(x)$ is determined from Progri(2021, [9] (15)) which is restricted to the inner segment of the absolute values of x less than or equal to x_0 as shown below

$$F_{in}(x) = \begin{vmatrix} 0.5 - \int_b^{2b-x} f(t)dt, & -x_0 < x \le b \\ 0.5 + \int_b^x f(t)dt\,, & b < x \le x_0 \end{vmatrix} \quad (39)$$

The *outer* cdf segment $F_{in}(x)$ is determined from Progri(2023, [16] (31)) which is restricted to the outer segment of the absolute values of x greater than or equal to x_0 as shown below

$$F_{ou}(x) = \begin{vmatrix} \int_{-\infty}^x f(t)dt\,, & x \le -x_0 \\ 1 - \int_x^{\infty} f(t)dt\,, & x > x_0 \end{vmatrix} \quad (40)$$

Instead of solving the general integral we will start with solving the special case solution (12); hence, the pdf is equal to (19).

3.1.1 First Special Case of the LHC of the GPCFD CDF

The first special case occurs when (12) and (19) occur.

Let us define the integral from b to x of $f(t)$ as $\mathcal{F}_{in}(x)$ which is written as

$$\mathcal{F}_{in}(x) = \int_b^x f(t)dt$$
$$= \int_b^x \frac{q_0(t)\Phi_c[z_0(t)] + q_1(t)\Phi_c[z_1(t)]}{\pi^{-0.5}2^{0.5}a^{-1}e^{\frac{-2a^2}{3c^4}}C} dt$$
$$= \frac{\int_b^x q_0(t)\Phi_c[z_0(t)]dt + \int_b^x q_1(t)\Phi_c[z_1(t)]dt}{\pi^{-0.5}2^{0.5}a^{-1}e^{\frac{-2a^2}{3c^4}}C}$$
$$= \frac{\mathcal{G}_{in}(x)}{\pi^{-0.5}2^{0.5}a^{-1}e^{\frac{-2a^2}{3c^4}}C} \quad (41)$$

where

$$\mathcal{G}_{in}(x) = \mathcal{G}_{in0}(x) + \mathcal{G}_{in1}(x) \quad (42)$$

Next, the integral $\mathcal{G}_{in0}(x)$ is split into two components: the $\mathcal{G}_{in0*}(x)$ or the star component that can be analytically integrated and a $\mathcal{G}_{in0\dagger}(x)$ which can only be integrated numerically as of this journal paper:

$$\mathcal{G}_{in0}(x) = \mathcal{G}_{in0*}(x) + \mathcal{G}_{in0\dagger}(x)$$
$$= \int_b^x e^{-\frac{1}{2}g_0^2(t)}\Phi_c[z_0(t)]dt$$
$$= \int_b^x e^{-\frac{1}{2}g_0^2(t)}\{1 - \Phi[z_0(t)]\}dt \quad (43)$$

The analytically integrated component $\mathcal{G}_{in0*}(x)$ is solved in Appen. B:

$$\mathcal{G}_{in0*}(x) = \int_b^x e^{-\frac{1}{2}g_0^2(t)}dt$$
$$= \sqrt{\frac{2}{3}}a\sqrt{\pi}\{\Phi(u_{x0}) - \Phi(u_0)\} \quad (44)$$

The numerically integrated component $\mathcal{G}_{in0\dagger}(x)$ is computed via the MATLAB integral built-in-function (BIF):

$$\mathcal{G}_{in0\dagger}(x) = -\int_b^x e^{-\frac{1}{2}g_0^2(t)}\Phi[z_0(t)]dt \quad (45)$$

Similarly, the integral $\mathcal{G}_{in1}(x)$ is split into two components: an analytically integrable component $\mathcal{G}_{in1*}(x)$ and into a numerically integrable component $\mathcal{G}_{in1\dagger}(x)$:

$$\mathcal{G}_{in1}(x) = \mathcal{G}_{in1*}(x) + \mathcal{G}_{in1\dagger}(x)$$
$$= \int_b^x e^{-\frac{1}{2}g_1^2(t)}\Phi_c[z_1(t)]dt$$
$$= \int_b^x e^{-\frac{1}{2}g_1^2(t)}\{1 - \Phi[z_1(t)]\}dt \quad (46)$$

The analytically integrable component, $\mathcal{G}_{in1*}(x)$, of the integral (46) is solved in Appen. C

$$\mathcal{G}_{in1*}(x) = \int_b^x e^{-\frac{1}{2}g_1^2(t)}dt$$
$$= \sqrt{\frac{2}{3}}a\sqrt{\pi}[\Phi(u_{x1}) + \Phi(u_0)] \quad (47)$$

$$\mathcal{G}_{in1\dagger}(x) = -\int_b^x e^{-\frac{1}{2}g_1^2(t)}\Phi[z_1(t)]dt \quad (48)$$

Next, from the definitions of Appen. B and C we obtain:

$$\mathcal{G}_{in}(x) = \mathcal{G}_{in*}(x) + \mathcal{G}_{in\dagger}(x) \quad (49)$$

$$\mathcal{G}_{in*}(x) = \mathcal{G}_{in0*}(x) + \mathcal{G}_{in1*}(x)$$
$$= \sqrt{\frac{2\pi}{3}}a\{\Phi(u_{x0}) - \Phi(u_0) + \Phi(u_{x1}) + \Phi(u_0)\}$$
$$= \sqrt{\frac{2\pi}{3}}a\{\Phi(u_{x0}) + \Phi(u_{x1})\} \quad (50)$$

$$\mathcal{G}_{in\dagger}(x) = \mathcal{G}_{in0\dagger}(x) + \mathcal{G}_{in1\dagger}(x)$$
$$= -\int_b^x \left[e^{-\frac{1}{2}g_0^2(t)}\Phi(z_0) + e^{-\frac{1}{2}g_1^2(t)}\Phi(z_1)\right]dt \quad (51)$$

Much to my surprise (51) cannon be simplified any further to yield faster computation than (51) as of the time this journal paper was completed. Equation (43) represents an LHC on the fastest computation of the GPCFD cdf.

This concludes the discussion on the first special case of the LHC of the GPCFD CDF.

3.1.2 Second Special Case of the GPCFD CDF

The second special case occurs when (23) and (34) occur.

Let us define the integral from b to x of $f(t)$ as $\mathcal{F}_{in}(x)$ which is written as

$$\mathcal{F}_{in}(x) = \int_b^x f(t)dt$$

$$= \int_b^x \frac{a^2\sqrt{\pi}\sum_{i=0}^{1} e^{\frac{z_i^2}{2}}\left[\frac{1}{\sqrt{\pi}}e^{-\frac{z_i^2}{2}} - \frac{1}{\sqrt{2}}z_i\Phi_c\left(\frac{z_i}{\sqrt{2}}\right) + \frac{4\Phi_c\left(\frac{z_i}{\sqrt{2}}\right)}{a\sqrt{2}}\right]}{d_0^{-1}(x)C}dt$$

$$= \frac{a\sum_{i=0}^{1}\int_b^x q_i(t)\left[\frac{1}{\sqrt{\pi}}e^{-\frac{z_i^2(t)}{2}} - \frac{1}{\sqrt{2}}z_i(t)\Phi_c\left[\frac{z_i(t)}{\sqrt{2}}\right] + \frac{4\Phi_c\left[\frac{z_i(t)}{\sqrt{2}}\right]}{a\sqrt{2}}\right]dt}{a^{-1}\pi^{-0.5}e^{\frac{-2a^2}{3c^4}}C}$$

$$= \frac{\mathcal{G}_{in}(x)}{\pi^{-0.5}a^{-2}e^{\frac{-2a^2}{3c^4}}C} \tag{52}$$

where $\mathcal{G}_{in}(x)$ is formed of two main integrals: $\mathcal{G}_{in0}(x)$ and $\mathcal{G}_{in1}(x)$ corresponding to the contributions coming from the integral whose components containing the zero and one subscripts respectively; however, the same is also made of two other integrals, the start (*) and dagger (†) components corresponding to the analytically and numerically integrable components as follows:

$$\mathcal{G}_{in}(x) = \mathcal{G}_{in0}(x) + \mathcal{G}_{in1}(x)$$

$$= \mathcal{G}_{in*}(x) + \mathcal{G}_{in\dagger}(x) \tag{53}$$

The start (*) and dagger (†) components are also made of the $\mathcal{G}_{in0*}(x)$ and $\mathcal{G}_{in1*}(x)$ corresponding to the contributions coming from the integral whose components containing the zero and one subscripts respectively

$$\mathcal{G}_{in*}(x) = \mathcal{G}_{in0*}(x) + \mathcal{G}_{in1*}(x) \tag{54}$$

$$\mathcal{G}_{in\dagger}(x) = \mathcal{G}_{in0\dagger}(x) + \mathcal{G}_{in1\dagger}(x) \tag{55}$$

Next, let us define the component associated with the zero subscript which is the sum of the start (*) and dagger (†) components as follows:

$$\mathcal{G}_{in0}(x) = \mathcal{G}_{in0*}(x) + \mathcal{G}_{in0\dagger}(x)$$

$$= \int_b^x e^{-\frac{1}{2}g_0^2(t)}\left[-\frac{z_0(t)\Phi_c\left[\frac{z_0(t)}{\sqrt{2}}\right]}{\sqrt{2}} + \frac{4\Phi_c\left[\frac{z_0(t)}{\sqrt{2}}\right]}{a\sqrt{2}}\right]dt \tag{56}$$

where the computation of either the start (*) and dagger (†) components is described in great detail

$$\mathcal{G}_{in0q}(x) = \sum_{i=1}^{3}\mathcal{G}_{in0iq}(x),\ q = \{*, \dagger\} \tag{57}$$

$$\mathcal{G}_{in01*}(x) = \int_b^x e^{-\frac{1}{2}g_0^2(t)}\frac{e^{-\frac{z_0^2(t)}{2}}}{\sqrt{\pi}}dt$$

$$= \frac{\int_b^x e^{-\frac{g_0^2(t)+z_0^2(t)}{2}}dt}{\sqrt{\pi}}$$

$$= \frac{a}{\sqrt{2}}e^{\frac{-2a^2}{3c^4}}\Phi(\upsilon_x) \tag{58}$$

$$\mathcal{G}_{in01\dagger}(x) = 0 \tag{59}$$

$$\mathcal{G}_{in02}(x) = \mathcal{G}_{in02*}(x) + \mathcal{G}_{in02\dagger}(x)$$

$$= -\int_b^x e^{-\frac{1}{2}g_0^2(t)}\frac{z_0(t)\Phi_c\left[\frac{z_0(t)}{\sqrt{2}}\right]}{\sqrt{2}}dt \tag{60}$$

$$\mathcal{G}_{in02*}(x) = -\int_b^x e^{-\frac{1}{2}g_0^2(t)}\frac{z_0(t)}{\sqrt{2}}dt$$

$$= -\frac{4\sqrt{\pi}a^2[\Phi(\theta_x)-\Phi(\theta_0)]}{3\sqrt{3}c^2} + \frac{\sqrt{2}a\left(e^{-\theta_0^2}-e^{-\theta_x^2}\right)}{3} \tag{61}$$

$$\mathcal{G}_{in02\dagger}(x) = \int_b^x e^{-\frac{1}{2}g_0^2(t)}\frac{z_0(t)\Phi\left[\frac{z_0(t)}{\sqrt{2}}\right]}{\sqrt{2}}dt \tag{62}$$

$$\mathcal{G}_{in03}(x) = \mathcal{G}_{in03*}(x) + \mathcal{G}_{in03\dagger}(x)$$

$$= \int_b^x e^{-\frac{1}{2}g_0^2(t)}\frac{4\Phi_c\left[\frac{z_0(t)}{\sqrt{2}}\right]}{a\sqrt{2}}dt \tag{63}$$

$$\mathcal{G}_{in03*}(x) = \frac{4\int_b^x e^{-\frac{1}{2}g_0^2(t)}dt}{a\sqrt{2}}$$

$$= \frac{4\sqrt{\pi}[\Phi(u_{x1})-\Phi(u_0)]}{\sqrt{3}} \tag{64}$$

$$\mathcal{G}_{in03\dagger}(x) = -\frac{4\int_b^x e^{-\frac{1}{2}g_0^2(t)}\Phi\left[\frac{z_0(t)}{\sqrt{2}}\right]dt}{a\sqrt{2}} \tag{65}$$

The details of the computation of the $\mathcal{G}_{in01*}(x)$ and $\mathcal{G}_{in02*}(x)$ components are given in Appen. D. However, the computation of $\mathcal{G}_{in03*}(x)$ is given in Appen. B.

Next, let us define the component associated with the one subscript which is the sum of the start (*) and dagger (†) components as follows:

$$\mathcal{G}_{in1}(x) = \mathcal{G}_{in1*}(x) + \mathcal{G}_{in1\dagger}(x)$$

$$= \int_b^x \frac{\frac{e^{-\frac{z_1^2(t)}{2}}}{\sqrt{\pi}} - \frac{z_1(t)\Phi_c\left[\frac{z_1(t)}{\sqrt{2}}\right]}{\sqrt{2}} + \frac{4\Phi_c\left[\frac{z_1(t)}{\sqrt{2}}\right]}{a\sqrt{2}}}{e^{\frac{1}{2}g_1^2(t)}}dt \tag{66}$$

Where the computations of either the start (*) and dagger (†) components associated with the one subscript are given as follows:

$$\mathcal{G}_{in1q}(x) = \sum_{i=1}^{3}\mathcal{G}_{in1iq}(x),\ q = \{*, \dagger\} \tag{67}$$

$$\mathcal{G}_{in11*}(x) = \int_b^x e^{-\frac{1}{2}g_1^2(t)}\frac{e^{-\frac{z_1^2(t)}{2}}}{\sqrt{\pi}}dt$$

$$= \frac{\int_b^x e^{-\frac{g_1^2(t)+z_1^2(t)}{2}}dt}{\sqrt{\pi}}$$

$$= \frac{a}{\sqrt{2}}e^{-\frac{2a^2}{3c^4}}\Phi(\upsilon_x) \tag{68}$$

$$\mathcal{G}_{in11\dagger}(x) = 0 \tag{69}$$

$$\mathcal{G}_{in12}(x) = \mathcal{G}_{in12*}(x) + \mathcal{G}_{in12\dagger}(x)$$

$$= -\int_b^x e^{-\frac{1}{2}g_1^2(t)}\frac{z_1(t)\Phi_c\left[\frac{z_1(t)}{\sqrt{2}}\right]}{\sqrt{2}}dt \tag{70}$$

$$\mathcal{G}_{in12*}(x) = -\int_b^x e^{-\frac{1}{2}g_1^2(t)}\frac{z_1(t)}{\sqrt{2}}dt$$

$$= -\frac{4\sqrt{\pi}a^2[\Phi(\delta_x)-\Phi(\delta_0)]}{3\sqrt{3}c^2} - \frac{\sqrt{2}a\left(e^{-\delta_0^2}-e^{-\delta_x^2}\right)}{3} \quad (71)$$

$$\mathcal{G}_{in12\dagger}(x) = \int_b^x e^{-\frac{1}{2}g_1^2(t)} \frac{z_1(t)\Phi\left[\frac{z_1(t)}{\sqrt{2}}\right]}{\sqrt{2}} dt \quad (72)$$

$$\mathcal{G}_{in13}(x) = \mathcal{G}_{in13*}(x) + \mathcal{G}_{in13\dagger}(x)$$

$$= \int_b^x e^{-\frac{1}{2}g_1^2(t)} \frac{4\Phi_c\left[\frac{z_1(t)}{\sqrt{2}}\right]}{a\sqrt{2}} dt \quad (73)$$

$$\mathcal{G}_{in13*}(x) = \frac{4\int_b^x e^{-\frac{1}{2}g_1^2(t)}dt}{a\sqrt{2}}$$

$$= \frac{4\sqrt{\pi}[\Phi(u_{x1})+\Phi(u_0)]}{\sqrt{3}} \quad (74)$$

$$\mathcal{G}_{in13\dagger}(x) = -\frac{4\int_b^x e^{-\frac{1}{2}g_1^2(t)}\Phi\left[\frac{z_1(t)}{\sqrt{2}}\right]dt}{a\sqrt{2}} \quad (75)$$

The details of the computation of the $\mathcal{G}_{in11*}(x)$ (68) and $\mathcal{G}_{in12*}(x)$ (71) components are given in Appen. E. However, the computation of $\mathcal{G}_{in03*}(x)$ (74) is given in Appen. B.

Next, the sum of the (*) components defined as the $\mathcal{G}_{in\Sigma1*}(x)$ is equal to twice the amount of either the (*) components associated with either the zero or one subscript as follows:

$$\mathcal{G}_{in\Sigma1*}(x) = \mathcal{G}_{in01*}(x) + \mathcal{G}_{in11*}(x)$$

$$= \frac{a}{\sqrt{2}} e^{\frac{-2a^2}{3c^4}} \Phi(v_x) + \frac{a}{\sqrt{2}} e^{-\frac{2a^2}{3c^4}} \Phi(v_x)$$

$$= \frac{2a}{\sqrt{2}} e^{\frac{-2a^2}{3c^4}} \Phi(v_x) \quad (76)$$

Next, the sum of the (*) components defined as the $\mathcal{G}_{in\Sigma2*}(x)$ is equal to the following:

$$\mathcal{G}_{in\Sigma2*}(x) = \mathcal{G}_{in02*}(x) + \mathcal{G}_{in12*}(x)$$

$$= -\frac{4\sqrt{\pi}a^2[\Phi(\theta_x)+\Phi(\delta_x)]}{3\sqrt{3}c^2} - \frac{\sqrt{2}a\left(e^{-\theta_x^2}-e^{-\delta_x^2}\right)}{3} \quad (77)$$

Next, the sum of the (*) components defined as the $\mathcal{G}_{in\Sigma3*}(x)$ is equal is equal to the following:

$$\mathcal{G}_{in\Sigma3*}(x) = \mathcal{G}_{in03*}(x) + \mathcal{G}_{in13*}(x)$$

$$= \frac{8\sqrt{\pi}\Phi(u_{x1})}{\sqrt{3}} \quad (78)$$

Next, the (*) component, $\mathcal{G}_{in*}(x)$, is equal to the sum of (76)-(78) as shown below:

$$\mathcal{G}_{in*}(x) = \mathcal{G}_{in0*}(x) + \mathcal{G}_{in1*}(x)$$

$$= \mathcal{G}_{in\Sigma1*}(x) + \mathcal{G}_{in\Sigma2*}(x) + \mathcal{G}_{in\Sigma3*}(x) \quad (79)$$

Next, the sum of the (†) components defined as the $\mathcal{G}_{in\Sigma1\dagger}(x)$ is equal to zero:

$$\mathcal{G}_{in\Sigma1\dagger}(x) = \mathcal{G}_{in01\dagger}(x) + \mathcal{G}_{in11\dagger}(x)$$

$$= 0 \quad (80)$$

Next, the sum of the (†) components defined as the $\mathcal{G}_{in\Sigma2\dagger}(x)$ is equal to the following:

$$\mathcal{G}_{in\Sigma2\dagger}(x) = \mathcal{G}_{in02\dagger}(x) + \mathcal{G}_{in12\dagger}(x)$$

$$= \int_b^x \frac{z_0(t)\Phi\left[\frac{z_0(t)}{\sqrt{2}}\right]}{\sqrt{2}e^{\frac{1}{2}g_0^2(t)}} dt + \int_b^x \frac{z_1(t)\Phi\left[\frac{z_1(t)}{\sqrt{2}}\right]}{\sqrt{2}e^{\frac{1}{2}g_1^2(t)}} dt \quad (81)$$

Next, the sum of the (†) components defined as the $\mathcal{G}_{in\Sigma3\dagger}(x)$ is equal is equal to the following:

$$\mathcal{G}_{in\Sigma3\dagger}(x) = \mathcal{G}_{in03\dagger}(x) + \mathcal{G}_{in13\dagger}(x)$$

$$= -\frac{4\int_b^x e^{-\frac{1}{2}g_0^2(t)}\Phi\left[\frac{z_0(t)}{\sqrt{2}}\right]dt}{a\sqrt{2}} - \frac{4\int_b^x e^{-\frac{1}{2}g_1^2(t)}\Phi\left[\frac{z_1(t)}{\sqrt{2}}\right]dt}{a\sqrt{2}} \quad (82)$$

Next, the (†) component, $\mathcal{G}_{in\dagger}(x)$, is equal to the sum of (80)-(82) as shown below:

$$\mathcal{G}_{in\dagger}(x) = \mathcal{G}_{in0\dagger}(x) + \mathcal{G}_{in1\dagger}(x)$$

$$= \mathcal{G}_{in\Sigma1\dagger}(x) + \mathcal{G}_{in\Sigma2\dagger}(x) + \mathcal{G}_{in\Sigma3\dagger}(x) \quad (83)$$

Finally, substituting (80) and (83) into (52) produces

$$\mathcal{F}_{in}(x) = \frac{\mathcal{G}_{in*}(x)+\mathcal{G}_{in\dagger}(x)}{\pi^{-0.5}a^{-2}e^{\frac{-2a^2}{3c^4}}C} \quad (84)$$

This concludes the discussion on the second special case of the LHC of the GPCFD CDF.

4 Numerical, Theoretical Results

In this section we compare and contrast the performance of the LHC of the GPCFD cdf with the Special Cases of the GPCFD cdf discussed in Progri (2021, [8]), LGPCFD cdf Progri (2021, [9]), and CGPCFD cdf Progri(2023, [16]). Significant improvements of the LHC of the GPCFD cdf are presented in SubSects. 4.1 and Examples in SubSects. 4.2.

4.1 Significant Improvement

Before we can discuss the examples in the numerical, theoretical result SubSect. 4.2, we first discuss the significant improvements in the computation of the GPCFD CDF.

First, the elimination of the linear approximation computation (LAC) that was last employed in Progri(2021, [8]-[10]). It was time to eliminate the LAC because it already served its purpose.

Second, for the first time the computation of the GPCFD CDF is split into segments for all the different methods of computation. The inner segment is significantly shorter than the outer segment.

Third, the computation of the outer segment is performed either via the MATLAB integral BIF or complementary GPCFD CDF Progri(2023, [16]).

Fourth, for the first time the computation of the inner segment is done either by means of the MATLAB integral BIF

TABLE I: THE TIME QUANTITATIVE COMPUTATIONAL PERFORMANCE

GPCDF cdf: CDF 1: Integral CDF 2 HLC GPCFD (41) + Integral CDF 3 SC GPCFD (153)-(159) + SC CLGPCFD (46) CDF 4 HLC GPCFD (41) + SC CLGPCFD (46)				
$a = 1, b = 1, N = 1, \sum(\cdot) = -, [120,120], [10,10]$				
CDF 1 (sec)	CDF 2 (sec)	CDF 3 (sec)	CDF 4 (sec)	Total (sec)
0.8971	0.8775	27.3387	0.3825	29.4958
0.8705	0.8570	27.1582	0.3823	29.2681
0.8862	0.9729	27.3150	0.3807	29.5548
0.8698	0.8558	27.2368	0.3838	29.3462
$a = 1.5, b = 1, N = 1, \sum(\cdot) = -, [120, 120], [10,10]$				
CDF 1 (sec)	CDF 2 (sec)	CDF 3 (sec)	CDF 4 (sec)	Total (sec)
0.9179	0.9489	31.5404	0.4331	33.8403
0.8874	0.8589	28.4124	0.4132	30.5718
0.9361	0.9119	28.3235	0.4157	30.5872
0.8861	0.8677	28.3471	0.4171	30.5180
$a = 2, b = 1, N = 1, \sum(\cdot) = -, [120, 120], [10,10]$				
CDF 1 (sec)	CDF 2 (sec)	CDF 3 (sec)	CDF 4 (sec)	Total (sec)
0.9245	0.9079	32.4075	0.5346	34.7746
0.9101	0.8659	30.4265	0.4423	32.6448
0.9155	0.8779	29.8927	0.4405	32.1267
0.9934	0.9328	31.2663	0.4510	33.6435

TABLE II: THE ACCURACY QUANTITATIVE COMPUTATIONAL PERFORMANCE

GPCFD cdf: CDF 1: Integral CDF 2 HLC GPCFD (41) + Integral CDF 3 SC GPCFD (153)-(159) + SC CLGPCFD (46) CDF 4 HLC GPCFD (41) + SC CLGPCFD (46)		
$a = 1, b = 1, N = 1, \sum(\cdot) = -, [120,100], [10,10]$		
CDF 1 − CDF 2 (f)	CDF 1 − CDF 3 (f)	CDF 1 − CDF 4 (f)
1.1657	10.2141	1.1657
$a = 1.5, b = 1, N = 1, \sum(\cdot) = -, [120, 100], [10,10]$		
CDF 1 − CDF 2 (f)	CDF 1 − CDF 3 (f)	CDF 1 − CDF 4 (f)
0.4441	2.6645	0.4441
$a = 2, b = 1, N = 1, \sum(\cdot) = -, [120, 100], [10,10]$		
CDF 1 − CDF 2 (f)	CDF 1 − CDF 3 (f)	CDF 1 − CDF 4 (f)
0.4441	2.3315	0.4441

or via the LHC of the GPCFD.

Fifth, for the first time the computation of the GPCFD does not involve the means of Kampé de Fériet function for the computation of the inner segment via the LHC of the GPCFD.

Sixth, we have doubled the number of points for the simulation test setup, and we have also included the negative points.

This concludes the discussion of the major improvements of the computation of the GPCFD cdf. Next, we consider a few examples.

4.2 Examples

The setup for the numerical examples is exactly the same as the one in Numerical Examples Sect. Progri (2021, [8]), Progri (2021, [9]), and Progri (2023, [16]).

We ran the simulations on a Dell computer Intel(R) Core(TM) i5-2400 CPU @ 3.10 GHz using MATLAB 2020b [18] using a vector of $-100 \leq x \leq 100$ with a sample increment of $\Delta x = 0.05$ that leads to 4000 points.

Table I presents the computational duration times in seconds for the first special case; i.e., for $N = 1$, of the cdf 1 or the integral, cdf 2 the HLC of the GPCFD cdf (41) for the inner plus integral cdf for the outer, cdf 3 is SC (153)-(159) of Progri (2021, [8]) for the inner plus SC CLGPCFD (46) Progri (2023, [16]) for the outer segment, and cdf 4 is HLC of the GPCFD cdf (41) for the inner plus the CLGPCFD (46) Progri (2023, [16]) for the outer segment.

The first four rows in Tab. 1 correspond to the computation times for values of $a = 1$; $b = 1$; $N = 1$ for cdf 3 $[120, 100]$ terms for option four that is used for the computation of the four pairs of the Kampé de Fériet functions (or double hypergeometric series) Progri (2018, [4] Appen. A) and eight Srivastava's Triple Hypergeometric Series $F^{(3)}[x, y, z]$ (see Appen. E of Progri (2019, [5]); and [10,10] terms employed in the computation of the two (or four) pairs of the Kampé de Fériet functions in (30) Progri(2023, [16]). In all of the run that we performed the computation for cdfs 3 and 4, I used option 4 in both the computation of the Kampé de Fériet functions and Srivastava's Triple Hypergeometric Series $F^{(3)}[x, y, z]$ (see Appen. E of Progri (2019, [5]).

The second and third four rows in Tab. I correspond to the same as the first four rows but for the value of $a = 1.5$ and $a = 2$ respectively. Based on the results of Tab. I, the computational time increases slightly as a function of the parameter a. The fastest computational time corresponds to the cdf 4, for $a = 1$ equal to 0.3807 and the slowest computational time corresponds to the cdf 3, for $a = 2$ equal to 32.4075 and all the remaining parameters the same. The ratio of the slowest vs. the fastest is equal to 85.1261 or almost two orders of magnitude slower. Hence, cdf 4 or HLC of the GPCFD cdf (41) for the inner plus the CLGPCFD (46) Progri (2023, [16]) is two orders of magnitude faster than cdf 3 is SC (153)-(159) of Progri (2021, [8]) for the inner plus SC

TABLE III: THE TIME QUANTITATIVE COMPUTATIONAL PERFORMANCE

GPCFD cdf: CDF 1: Integral CDF 2 HLC GPCFD (52) +Integral CDF 3 SC GPCFD (57) + SC CLGPCFD (54) CDF 4 HLC GPCFD (52) + SC CLGPCFD (54)				
$a = 1, b = 1, N = 2, \sum(\cdot) = -, [120, 120], [10,10]$				
CDF 1 (sec)	CDF 2 (sec)	CDF 3 (sec)	CDF 4 (sec)	Total (sec)
1.0018	1.1470	58.1152	0.7841	61.0482
1.0476	1.0743	59.1160	0.8024	62.0403
0.9696	1.0140	54.0611	0.7784	56.8232
1.0710	1.1384	55.6530	0.7943	58.6567
$a = 1.5, b = 1, N = 2, \sum(\cdot) = -, [120, 120], [10,10]$				
CDF 1 (sec)	CDF 2 (sec)	CDF 3 (sec)	CDF 4 (sec)	Total (sec)
0.9847	1.0366	56.3244	0.8299	59.1756
1.4933	1.2554	58.0089	0.8343	61.5918
1.1142	1.1634	57.8420	0.8368	60.9564
1.1160	1.1694	59.4754	0.9913	62.7521
$a = 2, b = 1, N = 2, \sum(\cdot) = -, [120, 120], [10,10]$				
CDF 1 (sec)	CDF 2 (sec)	CDF 3 (sec)	CDF 4 (sec)	Total (sec)
1.0011	1.0512	58.2087	0.8708	61.1318
1.1325	1.1561	60.1660	0.8732	63.3278
1.0114	1.1672	61.7617	0.8765	64.8168
0.9872	1.1808	59.6785	0.8880	62.7345

CLGPCFD (46) Progri (2023, [16]) for the outer segment.

Table II presents the accuracy quantitative computational performance corresponding to the cdfs 1 through 4 from the runs generated from Tab. I. In terms of accuracy, the computational errors of cdfs 1, 2 and 4 are the most accurate in order of femto[iv] or 10^{-15}; however, cdf 3 is one order of magnitude less accurate.

Table III is similar to Tab. I but for the second special case; i.e., $N = 2$; cdf 2 is (52) plus integral; cdf 3 is (57) plus (54); cdf 4 is (52) plus (54). The fastest computational time corresponds to the cdf 4, for $a = 1$ equal to 0.7784 and the slowest computational time corresponds to the cdf 3, for $a = 2$ equal to 61.7617 and all the remaining parameters the same. The ratio of the slowest vs. the fastest is equal to 79.3444 or almost two orders of magnitude slower. Cdf 4 is two orders of magnitude faster than cdf 3.

Table IV presents similar results from Tab. II but with the data coming from Tab. III. In terms of accuracy, the computational error of cdfs 1, 2 and 4 are the most accurate in order of femto[v] or 10^{-15}; however, cdf 3 is one to two orders of magnitude less accurate.

Hence, if we were to compare and contrast cdf 1, 3 with cdf 2, 4 is that they only have in common the outer segment.

TABLE IV: THE ACCURACY QUANTITATIVE COMPUTATIONAL PERFORMANCE

GPCFD cdf: CDF 1: Integral CDF 2 HLC GPCFD (52) +Integral CDF 3 SC GPCFD (57) + SC CLGPCFD (54) CDF 4 HLC GPCFD (52) + SC CLGPCFD (54)		
$a = 1, b = 1, N = 2, \sum(\cdot) = -, [120,120], [10,10]$		
CDF 1 − CDF 2 (f)	CDF 1 − CDF 3 (p)	CDF 1 − CDF 4 (f)
8.1601	1.9328	8.1601
$a = 1.5, b = 1, N = 2, \sum(\cdot) = -, [120, 120], [10,10]$		
CDF 1 − CDF 2 (f)	CDF 1 − CDF 3 (f)	CDF 1 − CDF 4 (f)
1.6098	42.0938	1.6098
$a = 2, b = 1, N = 2, \sum(\cdot) = -, [120, 120], [10,10]$		
CDF 1 − CDF 2 (f)	CDF 1 − CDF 3 (f)	CDF 1 − CDF 4 (f)
0.8882	12.4581	0.8882

However, cdf 2 and cdf 4 have only in common the inner segment. Cdf 1 and 3 do not have anything in common and neither do cdf 1 and 4.

Figure 1 (a) presents the GPCFD pdf and four GPCFD cdfs cdf 1 corresponds to the integral, cdf 2 the HLC of GPCFD cdf (41) plus Integral, (top), cdf 3 via EGPCFD (153)-(159) of Progri (2021, [8]) plus SC CLGPCFD (46) of Progri (2021, [16]), and cdf 4 HLC of GPCFD cdf (41) plus SC CLGPCFD (46) of Progri (2021, [16]) (bottom). In Fig. 1(b) the absolute error of the cdf 1 with cdf 2 is shown (top); and cdf 1 with cdf 3 and cdf 1 with cdf 4 (bottom).

Figure 2(a) and (b) present the same result as Fig. 1(a) and (b) but for values of $a = 1.5$; $b = 1$; $N = 1$.

Figure 3(a) and (b) present the same result as Fig. 1(a) and (b) but for values of $a = 2$; $b = 1$; $N = 1$.

Figure 4 (a) presents the GPCFD pdf and four GPCFD cdfs cdf 1 corresponds to the integral, cdf 2 the HLC of GPCFD cdf (52) plus Integral, (top), cdf 3 via EGPCFD (55) of Progri (2021, [8]) plus SC CLGPCFD (54) of Progri (2021, [16]), and cdf 4 HLC of GPCFD cdf (52) plus SC CLGPCFD (54) of Progri (2021, [16]) (bottom). In Fig. 1(b) the absolute error of the cdf 1 with cdf 2 is shown (top); and cdf 1 with cdf 3 and cdf 1 with cdf 4 (bottom).

Figure 5(a) and (b) present the same result as Fig. 4(a) and (b) but for values of $a = 1.5$; $b = 1$; $N = 2$.

Figure 6(a) and (b) present the same result as Fig. 4(a) and (b) but for values of $a = 2$; $b = 1$; $N = 2$.

This concluded the discussion on examples and numerical, theoretical results.

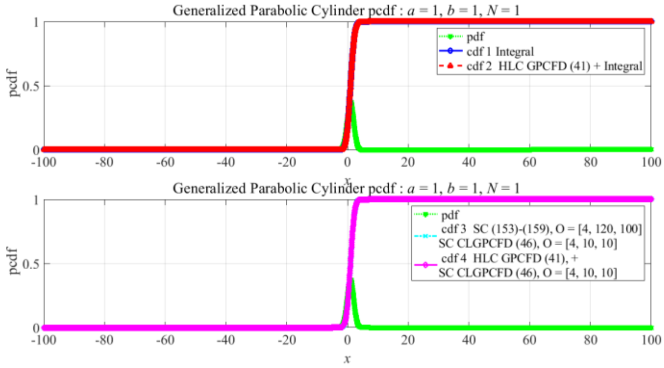

(a) The computation of the GPCFD pdf and cdf for $-100 \leq x \leq 100$, $a = 1$, $b = 1$, $N = 1$.

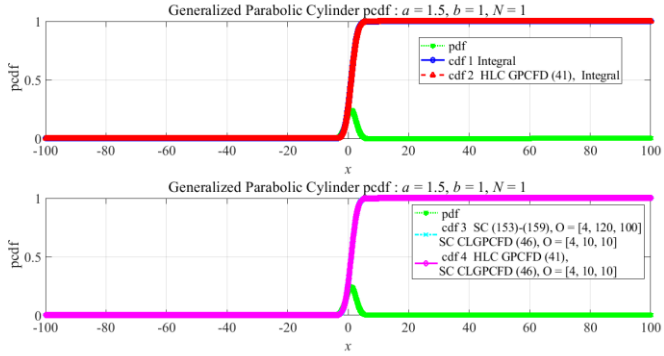

(a) The computation of the GPCFD pdf and cdf for $-100 \leq x \leq 100$, $a = 1.5$, $b = 1$, $N = 1$.

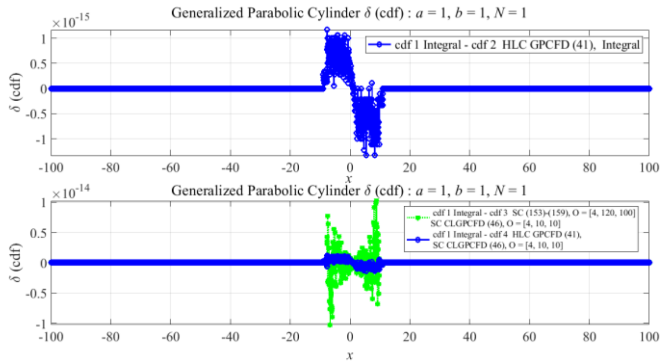

(b) The absolute error the GPCFD cdf for $-100 \leq x \leq 100$, $a = 1$, $b = 1$, $N = 1$.

Fig. 1. The computation of the GPCFD pdf and cdf for $-100 \leq x \leq 100$, $a = 1$, $b = 1$, $N = 1$.

Cdf 1 Integral

Cdf 2 the HLC GPCFD cdf (41) plus Integral BIF

Cdf 3 via SC EGPCFD (153)-(159) of Progri (2021, [10][8]) plus SC CLGPCFD (46)

Cdf 4 the HLC GPCFD cdf (41) plus SC CLGPCFD (46).

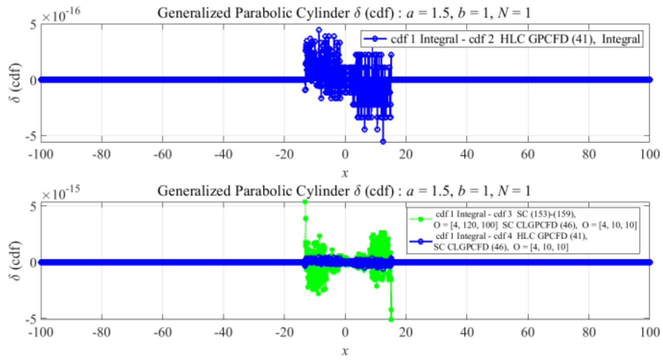

(b) The absolute error the GPCFD cdf for $-100 \leq x \leq 100$, $a = 1.5$, $b = 1$, $N = 1$.

Fig. 2. The computation of the GPCFD pdf and cdf for $-100 \leq x \leq 100$, $a = 1.5$, $b = 1$, $N = 1$.

Cdf 1 Integral

Cdf 2 the HLC GPCFD cdf (41) plus Integral BIF

Cdf 3 via SC EGPCFD (153)-(159) of Progri (2021, [10][8]) plus CLGPCFD (46)

Cdf 4 the HLC GPCFD cdf (41) plus CLGPCFD (46).

5 Conclusions

There are a lot of major accomplishments that need to be enumerated in this journal paper.

For the first time we have discussed the LHC of the GPCFD cdf which consists of two segments: the inner segment and the outer segment which is superior in computational time performance and accuracy compared to the MATLAB BIF or the SC (153)-(159) of Progri (2021, [8]) for the inner plus SC CLGPCFD (46) Progri (2023, [16]) for the outer segment using a vector of $-100 \leq x \leq 100$ with a sample increment of $\Delta x = 0.05$ that leads to 4000 points.

Cdf 4 or HLC of the GPCFD cdf (41) for the inner plus the CLGPCFD (46) Progri (2023, [16]) is two orders of magnitude faster than cdf 3 is SC (153)-(159) of Progri (2021, [8]) for the inner plus SC CLGPCFD (46) Progri (2023, [16]) for the outer segment.

The computational errors of cdfs 1, 2 and 4 are the most accurate in order of femto or 10^{-15}; however, cdf 3 or the SC (153)-(159) of Progri (2021, [8]) for the inner plus SC CLGPCFD (46) Progri (2023, [16]) is one order of magnitude less accurate.

This work represents a major milestone in comparison to the work performed in Progri (2021, [8]) and Progri (2023, [16]).

In a separate publication we will examine what happens when $b = 0$ and what happens when $-\infty < a, b, c < 0$.

6 Acknowledgement

This work was supported by Giftet Inc. executive office.

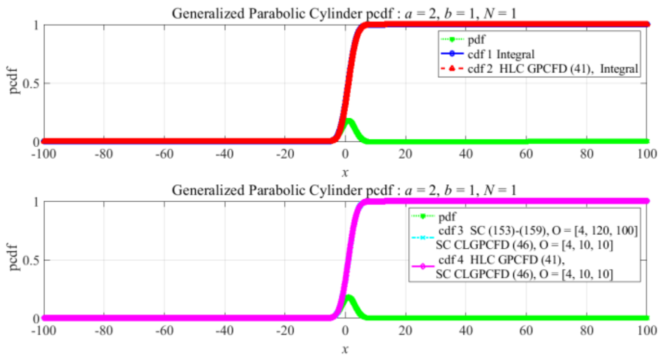

(a) The computation of the GPCFD pdf and cdf for $-100 \leq x \leq 100$, $a = 2$, $b = 1$, $N = 1$.

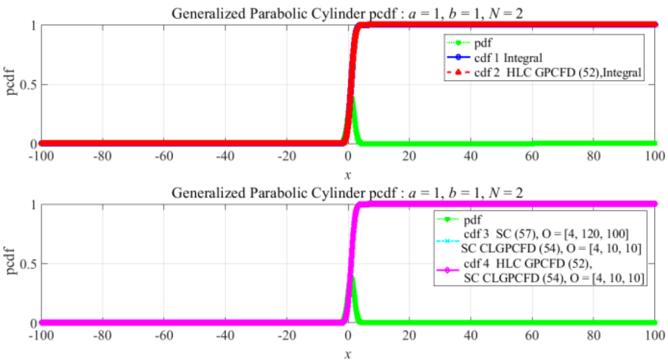

(a) The computation of the GPCFD pdf and cdf for $-100 \leq x \leq 100$, $a = 1$, $b = 1$, $N = 2$.

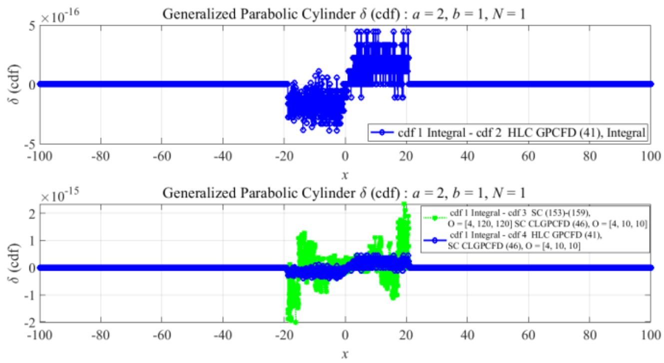

(b) The absolute error the GPCFD cdf for $-100 \leq x \leq 100$, $a = 2$, $b = 1$, $N = 1$.

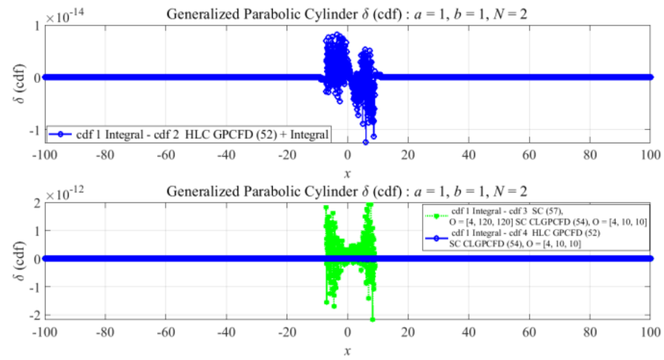

(b) The absolute error the GPCFD cdf for $-100 \leq x \leq 100$, $a = 1$, $b = 1$, $N = 2$.

Fig. 3. The computation of the GPCFD pdf and cdf for $-100 \leq x \leq 100$, $a = 2$, $b = 1$, $N = 1$.
Cdf 1 Integral
Cdf 2 the HLC GPCFD cdf (41) plus Integral BIF
Cdf 3 via SC EGPCFD (153)-(159) of Progri (2021, [10][8]) plus CLGPCFD (46)
Cdf 4 the HLC GPCFD cdf (41) plus CLGPCFD (46).

Fig. 4. The computation of the GPCFD pdf and cdf for $-100 \leq x \leq 100$, $a = 1$, $b = 1$, $N = 2$.
Cdf 1 Integral
Cdf 2 the HLC GPCFD cdf (52) plus Integral BIF
Cdf 3 via SC EGPCFD (57) of Progri (2021, [10][8]) plus SC CLGPCFD (54)
Cdf 4 the HLC GPCFD cdf (52) plus SC CLGPCFD (54).

I want to profoundly thank the MathWorks at Natick, Massachusetts for providing a sponsored MATLAB licence [18] to Giftet Inc. as part of the Indoor Geolocation Systems MATLAB Library development that will enable the results of this work to be published in Dr. Progri pioneer publication *Indoor Geolocation Systems—Theory and Applications. Vol. I* (Not yet available in print) [17].

This journal paper is dedicated to four special men in my life: my grandfather, Xhevdet Progri, my dear father, Fiqiri Progri, my father's first cousin Dr. Peter Demir, and Qazim Demir, the brother of my grandfather, Xhevdet Progri.

This journal paper is also dedicated to the Golden Bear, Jack Nicklaus, the greatest golfer of all time. Needless to say I have fallen in love with his masterpiece book, *Golf My Way*. Moreover, Jack Nicklaus [18] reminds me of my grandfather who I loved very much.

Finally, I am also dedicating this journal paper to our most beloved President Ronald Reagan, who reminds me of my grandfather, [19] who spoke from the heart, who spoke the truth, who was a staunch supporter of personal freedom, the greatest leader of the free world, and perhaps the greatest critic of the wasteful government control and spending[vi].

"*Government is not the answer, government is the problem.*"—Ronald Reagan

I would like to express my deepest gratitude to my mother Lumturi Progri, my sister Adriana Dine, and Ms. Elizabeth Demir for their support, loyally, and dedication to me during some of the most difficult times in my life as a boy, man, and scholar.

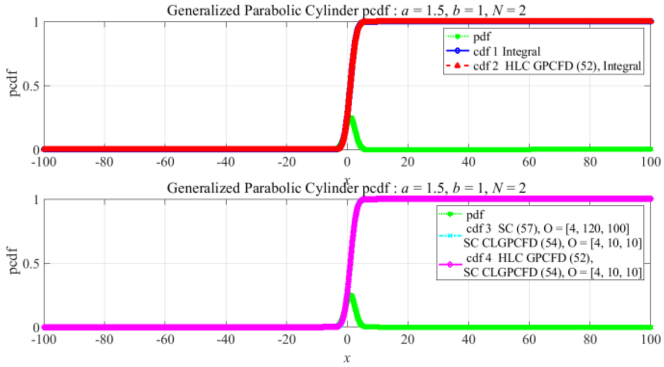

(a) The computation of the GPCFD pdf and cdf for $-100 \leq x \leq 100$, $a = 1.5$, $b = 1$, $N = 2$.

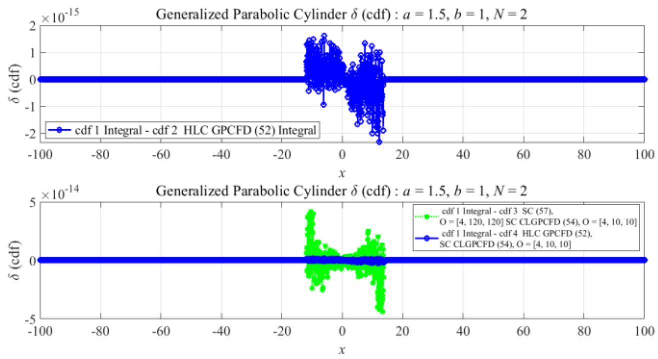

(b) The absolute error the GPCFD cdf for $-100 \leq x \leq 100$, $a = 1.5$, $b = 1$, $N = 2$.

Fig. 5. The computation of the GPCFD pdf and cdf for $-100 \leq x \leq 100$, $a = 1.5$, $b = 1$, $N = 2$.

Cdf 1 Integral

Cdf 2 the HLC GPCFD cdf (52) plus Integral BIF

Cdf 3 via SC EGPCFD (57) of Progri (2021, [10][8]) plus CLGPCFD (46)

Cdf 4 the HLC GPCFD cdf (52) plus CLGPCFD (54).

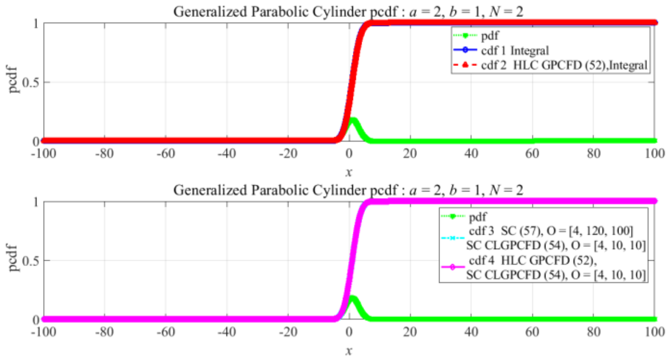

(a) The computation of the GPCFD pdf and cdf for $-100 \leq x \leq 100$, $a = 2$, $b = 1$, $N = 2$.

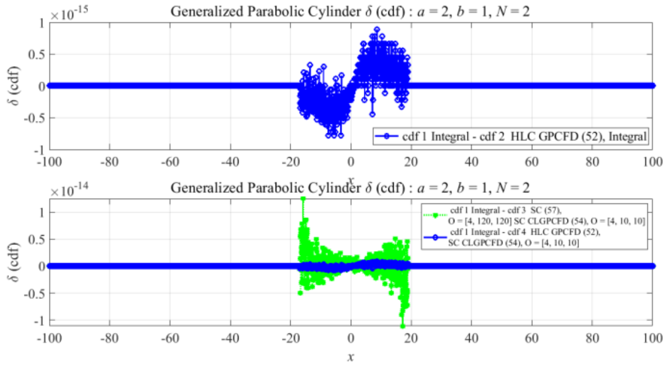

(b) The absolute error the GPCFD cdf for $-100 \leq x \leq 100$, $a = 2$, $b = 1$, $N = 2$.

Fig. 6. The computation of the GPCFD pdf and cdf for $-100 \leq x \leq 100$, $a = 2$, $b = 1$, $N = 2$.

Cdf 1 Integral

Cdf 2 the HLC GPCFD cdf (52) plus Integral BIF

Cdf 3 via SC EGPCFD (57) of Progri (2021, [10][8]) plus CLGPCFD (54)

Cdf 4 the HLC GPCFD cdf (52) plus CLGPCFD (54).

7 References

[1] I.S. Gradshteyn, I.M. Ryzhik, (A. Jeffrey, D. Zwillinger, editors) *Table of Integrals, Series, and Products*, 7th ed., Burlington, MA: Academic Press, 1171 pg., 2007.

[2] Anon., "Parabolic cylinder function," *Wikipedia, the free encyclopedia*, Apr. 2015, https://en.wikipedia.org/wiki/Parabolic_cylinder_function.

[3] I.F. Progri, "Generalized parabolic cylinder function distribution," vol. 2016, article ID 2016071605, 14 pg., Nov. 2016. DOI: https://doi.org/10.18610/JG3.2016.071605

[4] I.F. Progri, "Efficient computation of generalized Bessel function distributions," *J. Geol. Geoinfo. Geointel.*, vol. 2018, article ID 2018071604, 12 pg., Nov. 2018. DOI: https://doi.org/10.18610/JG3.2018.071605

[5] I.F. Progri, "Efficient computation of the special cases of the generalized Bessel function distributions," *J. Geol. Geoinfo. Geointel.*, vol. 2019, article ID 2019071601, 31 pg., Nov. 2019. DOI: https://doi.org/10.18610/JG3.2019.071601

[6] I.F. Progri, "The computation of a 2F2 hypergeometric function," *J. Geol. Geoinfo. Geointel.*, vol. 2020, article ID 2020071601, 12 pg., Nov. 2020. DOI: https://doi.org/10.18610/JG3.2020.071601

[7] I.F. Progri, "Confluent hypergeometric function irregular singularities," vol. 2021, article ID 2021071601, 12 pg., Nov. 2021. DOI: https://doi.org/10.18610/JG3.2021.071601

[8] I.F. Progri, "Efficient computation of the generalized parabolic cylinder function distribution," vol. 2021, article ID 2021071602, 17 pg., Nov. 2021. DOI: https://doi.org/10.18610/JG3.2021.071602

[9] I.F. Progri, "Landmark computation of the generalized parabolic cylinder function distribution," vol. 2021, article ID 2021071603, 15 pg., Nov. 2021. DOI: https://doi.org/10.18610/JG3.2021.071603

[10] I.F. Progri, "Special cases of the generalized parabolic cylinder function distribution," vol. 2021, article ID 2021071604, 12 pg., Nov. 2021. DOI: https://doi.org/10.18610/JG3.2021.071604

[11] I.F. Progri, "A study of the computation of the exponential function," *J. Geol. Geoinfo. Geointel.,* vol. 2022, article ID 2022071602, 10 pg., Nov. 2022. DOI: https://doi.org/10.18610/JG3.2022.071602

[12] I.F. Progri, "Landmark computation of the incomplete gamma function," *J. Geol. Geoinfo. Geointel.,* vol. 2022, article ID 2022071603, 16 pg., Nov. 2022. DOI: https://doi.org/10.18610/JG3.2022.071603

[13] I.F. Progri, "Landmark computation of the generalized Bessel function distributions of the first kind: part 2," *J. Geol. Geoinfo. Geointel.,* vol. 2022, article ID 2022071604, 14 pg., Nov. 2022. DOI: https://doi.org/10.18610/JG3.2022.071604

[14] I.F. Progri, "The significance of the landmark computations of the generalized Bessel function distribution of the first kind," *J. Geol. Geoinfo. Geointel.,* vol. 2022, article ID 2022071605, 7 pg., Nov. 2022. DOI: https://doi.org/10.18610/JG3.2022.071605

[15] I.F. Progri, "On the computation of the landmark generating function of the Hermite Polynomials," *J. Geol. Geoinfo. Geointel.,* vol. 2023, article ID 2023071603, 12 pg., Nov. 2023. DOI: https://doi.org/10.18610/JG3.2023.071603

[16] I.F. Progri, "Computation of the complementary landmark generalized Parabolic Cylinder Function distribution," *J. Geol. Geoinfo. Geointel.,* vol. 2023, article ID 2023071604, 17 pg., Nov. 2023. DOI: https://doi.org/10.18610/JG3.2023.071604

[17] I. Progri, *Indoor Geolocation Systems—Theory and Applications*. *Vol. I*, 1st ed., Worcester, MA: Giftet Inc., ~800 pp., ~ 2024 (not yet available in print).

[18] Anon., "Jack Nicklaus," *Wikipedia, the free encyclopedia*, June 2024. https://en.wikipedia.org/wiki/Jack_Nicklaus

[19] Anon., "Ronald Reagan," *Wikipedia, the free encyclopedia*, June 2024. https://en.wikipedia.org/wiki/Ronald_Reagan

[20] Anon, "MATLAB 2023b," *The MathWorks, Inc.*, Natick, MA, Copyright © 1994-2024. The MathWorks, Inc., https://mathworks.com/products/matlab.html

8 Appendix A: A Detailed Discussion of the GPCFD PDF Main Parameters

In Progri(2016, [3]), Progri(2021, [8]-[10]), Progri(2023, [14], [16]) (1) I made the statement that $-\infty < a, b, c < \infty$ and that $N \geq 1$ positive integer. We can safely assume that $N \geq 1$ is a positive integer. We can also safely assume that for $0 < a, b, c < \infty$ then either (1) is a valid pdf in that;

$$f(x) \geq 0 \tag{85}$$

$$\int_{-\infty}^{\infty} f(x) = 1 \tag{86}$$

Let us assume that

$$a = 0 \Rightarrow c = 0 \Rightarrow a_0(x) \rightarrow \infty \Rightarrow d_0(x) \rightarrow 0 \tag{87}$$

What happens to the ratio of $a/c^2 \rightarrow 0$? From the L'Hôpital's rule we have the following:

$$\frac{a}{c^2} \rightarrow 0 \tag{88}$$

Let us also assume that $N = 1$

$$f(x) = \frac{e^{-\frac{1}{2}\left[\frac{\sqrt{3}(x-b)}{2a}+\frac{a}{\sqrt{3}c^2}\right]^2}\Phi_c\left(\frac{z_0}{\sqrt{2}}\right)+e^{-\frac{1}{2}\left[\frac{\sqrt{3}(x-b)}{2a}-\frac{a}{\sqrt{3}c^2}\right]^2}\Phi_c\left(\frac{z_1}{\sqrt{2}}\right)}{\frac{2\sqrt{2}a\sqrt{\pi}\Phi_c\left(\frac{\sqrt{2}a}{\sqrt{3}c^2}\right)}{\sqrt{3}}} \tag{89}$$

Again, if we were to use the L'Hôpital's rule we will obtain the following:

$$f(x) = 0, \text{ iff } a = 0 \tag{90}$$

In other words, the parameter a cannot be equal to zero for the GPCFD pdf to satisfy the conditions (85) and (86). The same can be said about the parameter c. The parameter c cannot be equal to zero also because that would lead to (90). It only remains to examine the parameter b.

In a separate publication we will examine what happens when $b = 0$ and what happens when $-\infty < a, b, c < 0$.

This concludes the brief discussion on the GPCDF main parameters.

9 Appendix B: The Derivations of Integral (44)

In order to derive the integral (44) we obtain the following:

$$\int_b^x e^{-\frac{1}{2}g_0^2(t)} dt = \int_b^x e^{-\frac{3}{2}\left(\frac{t-b}{2a}+\frac{a}{3c^2}\right)^2} dt$$

$$= \int_b^x e^{-u^2} \sqrt{\frac{2}{3}} 2adu$$

$$= \sqrt{\frac{2}{3}} 2a \int_{u_0}^{u_x} e^{-u^2} du$$

$$= \sqrt{\frac{2}{3}} a\sqrt{\pi} \Phi(u)\Big|_{u_0}^{u_{x0}}$$

$$= \sqrt{\frac{2}{3}} a\sqrt{\pi} [\Phi(u_{x0}) - \Phi(u_0)] \tag{91}$$

First, we make the substitution

$$u = \sqrt{\frac{3}{2}} \left(\frac{t-b}{2a} + \frac{a}{3c^2}\right) \Rightarrow du = \sqrt{\frac{3}{2}} \frac{dt}{2a} \Rightarrow dt = \sqrt{\frac{2}{3}} 2adu \tag{92}$$

$$t \to \Big|_b^x \Rightarrow u \to \Big|_{\sqrt{\frac{3}{2}\frac{a}{3c^2}} = u_0}^{\sqrt{\frac{3}{2}}\left(\frac{x-b}{2a} + \frac{a}{3c^2}\right) = u_{x0}} \tag{93}$$

$$a\left[\frac{1}{c^2} - a_0(t)\right] = \frac{a}{c^2} - \frac{t-b}{2a} = \frac{2a}{3c^2} - \sqrt{\frac{2}{3}} u \tag{94}$$

This completes the solution of the integral (44).

10 Appendix C: The Deduction of Integral (47)

The deduction of the integral (47) is produced from the following:

$$\int_b^x e^{-\frac{1}{2} g_1^2(t)} dt = \int_b^x e^{-\frac{3}{2}\left(\frac{t-b}{2a} - \frac{a}{3c^2}\right)^2} dt$$

$$= \int_b^x e^{-u^2} \sqrt{\frac{2}{3}} 2adu$$

$$= \sqrt{\frac{2}{3}} 2a \int_{u_0}^{u_{x1}} e^{-u^2} du$$

$$= \sqrt{\frac{2}{3}} a\sqrt{\pi} \Phi(u)\Big|_{-u_0}^{u_{x1}}$$

$$= \sqrt{\frac{2}{3}} a\sqrt{\pi} [\Phi(u_{x1}) - \Phi(-u_0)]$$

$$= \sqrt{\frac{2}{3}} a\sqrt{\pi} [\Phi(u_{x1}) + \Phi(u_0)] \tag{95}$$

First, we make the substitution

$$u = \sqrt{\frac{3}{2}} \left(\frac{t-b}{2a} - \frac{a}{3c^2}\right) \Rightarrow du = \sqrt{\frac{3}{2}} \frac{dt}{2a} \Rightarrow dt = \sqrt{\frac{2}{3}} 2adu \tag{96}$$

$$t \to \Big|_b^x \Rightarrow u \to \Big|_{-\sqrt{\frac{3}{2}\frac{a}{3c^2}} = -u_0}^{\sqrt{\frac{3}{2}}\left(\frac{x-b}{2a} - \frac{a}{3c^2}\right) = u_{x1}} \tag{97}$$

$$a\left[\frac{1}{c^2} - a_0(t)\right] = \frac{a}{c^2} - \frac{t-b}{2a} = \frac{2a}{3c^2} - \sqrt{\frac{2}{3}} u \tag{98}$$

This completes the deduction of the integral (47).

11 Appendix D: The Details of Integrals (58) and (61)

The details of the integral (58) lead to the following:

$$\int_b^x e^{-\frac{g_0^2(t) + z_0^2(t)}{2}} dt = \int_b^x e^{-\frac{3}{2}\left(\frac{t-b}{2a} + \frac{a}{3c^2}\right)^2 - \frac{a^2}{2}\left[\frac{1}{c^2} - \frac{(t-b)}{2a^2}\right]^2} dt$$

$$= \int_b^x e^{-\frac{(t-b)^2}{2a^2} - \frac{2a^2}{3c^4}} dt$$

$$= e^{-\frac{2a^2}{3c^4}} \int_b^x e^{-\frac{(t-b)^2}{2a^2}} dt$$

$$= e^{-\frac{2a^2}{3c^4}} \int_0^{v_x} e^{-v^2} \sqrt{2} adv$$

$$= \sqrt{2} a e^{-\frac{2a^2}{3c^4}} \int_0^{v_x} e^{-v^2} dv$$

$$= \sqrt{2} a e^{-\frac{2a^2}{3c^4}} \frac{\sqrt{\pi}}{2} \Phi(v)\Big|_0^{v_x}$$

$$= a\sqrt{\frac{\pi}{2}} e^{-\frac{2a^2}{3c^4}} \Phi(v_x) \tag{99}$$

Let us look at the solution of the simplifications of the numerator.

$$\frac{3}{2}\left(\frac{t-b}{2a} + \frac{a}{3c^2}\right)^2 + \frac{a^2}{2}\left[\frac{1}{c^2} - \frac{(t-b)}{2a^2}\right]^2 = \frac{(t-b)^2}{2a^2} + \frac{2a^2}{3c^4} \tag{100}$$

First, we make the substitution

$$v = \frac{t-b}{\sqrt{2}a} \Rightarrow dv = \frac{dt}{\sqrt{2}a} \Rightarrow dt = \sqrt{2} adv \tag{101}$$

$$t \to \Big|_b^x \Rightarrow v \to \Big|_0^{\frac{x-b}{\sqrt{2}a} = v_x} \tag{102}$$

Second, the integral (61) is solved by means of the following substitution

$$\frac{\int_b^x e^{\frac{-g_0^2(t)}{2}} z_0(t) dt}{\sqrt{2}} = \frac{\int_b^x e^{-\frac{3}{2}\left(\frac{t-b}{2a} + \frac{a}{3c^2}\right)^2} \left(\frac{4a}{3c^2} - \frac{t-b}{2a} - \frac{a}{3c^2}\right) dt}{\sqrt{2}}$$

$$= \frac{4a \int_b^x \frac{dt}{e^{\frac{3}{2}\left(\frac{t-b}{2a} + \frac{a}{3c^2}\right)^2}}}{3\sqrt{2}c^2} - \frac{\int_b^x \frac{\frac{\sqrt{3}}{\sqrt{2}}\left(\frac{t-b}{2a} + \frac{a}{3c^2}\right)}{e^{\frac{3}{2}\left(\frac{t-b}{2a} + \frac{a}{3c^2}\right)^2}} dt}{\sqrt{3}}$$

$$= \frac{8a^2 \int_{\theta_0}^{\theta_x} e^{-\theta^2} d\theta}{3\sqrt{3}c^2} + \frac{\sqrt{2}a \int_{\theta_0}^{\theta_x} e^{-\theta^2} d(-\theta^2)}{3}$$

$$= \frac{4\sqrt{\pi}a^2[\Phi(\theta_x)-\Phi(\theta_0)]}{3\sqrt{3}c^2} + \frac{\sqrt{2}a\int_{\theta_0}^{\theta_x} e^{-\theta^2} d(-\theta^2)}{3}$$

$$= \frac{4\sqrt{\pi}a^2[\Phi(\theta_x)-\Phi(\theta_0)]}{3\sqrt{3}c^2} - \frac{\sqrt{2}a\left(e^{-\theta_0^2}-e^{-\theta_x^2}\right)}{3} \quad (103)$$

Third, we make the substitution

$$\theta = \frac{\sqrt{3}}{\sqrt{2}}\left(\frac{t-b}{2a} + \frac{a}{3c^2}\right) \Rightarrow d\theta = \frac{\sqrt{3}}{\sqrt{2}}\frac{dt}{2a} \Rightarrow dt = \frac{2\sqrt{2}a}{\sqrt{3}}d\theta \quad (104)$$

$$t \to |_b^x \Rightarrow \theta \to |_{\frac{a}{\sqrt{6}c^2}=\theta_0}^{\frac{\sqrt{3}}{\sqrt{2}}\left(\frac{t-b}{2a}+\frac{a}{3c^2}\right)=\frac{\sqrt{3}}{2}\frac{(t-b)}{\sqrt{2}a}+\frac{a}{\sqrt{6}c^2}=\theta_x} \quad (105)$$

In conclusion we produced the CFE of the integrals (58) and (61). This concludes the derivations of Appen. D.

12 Appendix E: The Ingredients of Integral (68) and (71)

The ingredients of the integral (68) constitute the following:

$$\int_b^x e^{-\frac{g_1^2(t)+z_1^2(t)}{2}} dt = \int_b^x e^{-\frac{3}{2}\left(\frac{t-b}{2a}-\frac{a}{3c^2}\right)^2-\frac{a^2}{2}\left[\frac{1}{c^2}+\frac{(t-b)}{2a^2}\right]^2} dt$$

$$= \int_b^x e^{-\frac{(t-b)^2}{2a^2}+\frac{2a^2}{3c^4}} dt$$

$$= e^{-\frac{2a^2}{3c^4}}\int_b^x e^{-\frac{(t-b)^2}{2a^2}} dt$$

$$= e^{-\frac{2a^2}{3c^4}}\int_0^{\upsilon_x} e^{-\upsilon^2}\sqrt{2}a d\upsilon$$

$$= \sqrt{2}ae^{-\frac{2a^2}{3c^4}}\int_0^{\upsilon_x} e^{-\upsilon^2} d\upsilon$$

$$= \sqrt{2}ae^{-\frac{2a^2}{3c^4}}\frac{\sqrt{\pi}}{2}\Phi(u)|_0^{\upsilon_x}$$

$$= a\sqrt{\frac{\pi}{2}}e^{-\frac{2a^2}{3c^4}}\Phi(\upsilon_x) \quad (106)$$

Let us look at the solution of the simplifications of the numerator.

$$\frac{3}{2}\left(\frac{t-b}{2a} - \frac{a}{3c^2}\right)^2 + \frac{a^2}{2}\left[\frac{1}{c^2} + \frac{(t-b)}{2a^2}\right]^2 = \frac{(t-b)^2}{2a^2} + \frac{2a^2}{3c^4} \quad (107)$$

First, we make the substitution

$$\upsilon = \frac{t-b}{\sqrt{2}a} \Rightarrow d\upsilon = \frac{dt}{\sqrt{2}a} \Rightarrow dt = \sqrt{2}a d\upsilon \quad (108)$$

$$t \to |_b^x \Rightarrow \upsilon \to |_0^{\frac{x-b}{\sqrt{2}a}=\upsilon_x} \quad (109)$$

Second, we solve the following integral

$$\frac{\int_b^x e^{-\frac{1}{2}g_1^2(t)}z_1(t)dt}{\sqrt{2}} = \frac{\int_b^x e^{-\frac{3}{2}\left(\frac{t-b}{2a}-\frac{a}{3c^2}\right)^2} a\left[\frac{4}{3c^2}+\frac{(t-b)}{2a^2}-\frac{a}{3c^2}\right]dt}{\sqrt{2}}$$

$$= \frac{4a}{\sqrt{2}}\frac{\int_b^x \frac{dt}{e^{\frac{3}{2}\left(\frac{t-b}{2a}-\frac{a}{3c^2}\right)^2}}}{3c^2} + \frac{\int_b^x \frac{\frac{\sqrt{3}}{\sqrt{2}}\left(\frac{t-b}{2a}-\frac{a}{3c^2}\right)}{e^{\frac{3}{2}\left(\frac{t-b}{2a}-\frac{a}{3c^2}\right)^2}}dt}{\sqrt{3}}$$

$$= \frac{8a^2}{3\sqrt{3}c^2}\int_{\delta_0}^{\delta_x} e^{-\delta^2} d\delta - \frac{\sqrt{2}a}{3}\int_{\delta_0}^{\delta_x} e^{-\delta^2} d(-\delta^2)$$

$$= \frac{4\sqrt{\pi}a^2[\Phi(\delta_x)-\Phi(\delta_0)]}{3\sqrt{3}c^2} - \frac{\sqrt{2}a}{3}\int_{\delta_0}^{\delta_x} e^{-\delta^2} d(-\delta^2)$$

$$= \frac{4\sqrt{\pi}a^2[\Phi(\delta_x)-\Phi(\delta_0)]}{3\sqrt{3}c^2} + \frac{\sqrt{2}a\left(e^{-\delta_0^2}-e^{-\delta_x^2}\right)}{3} \quad (110)$$

Third, we make the substitution

$$\delta = \frac{\sqrt{3}}{\sqrt{2}}\left(\frac{t-b}{2a} - \frac{a}{3c^2}\right) \Rightarrow d\delta = \frac{\sqrt{3}}{\sqrt{2}}\frac{dt}{2a} \Rightarrow dt = \frac{2\sqrt{2}a}{\sqrt{3}}d\delta \quad (111)$$

$$t \to |_b^x \Rightarrow \delta \to |_{\frac{-a}{\sqrt{6}c^2}=\delta_0}^{\frac{\sqrt{3}}{\sqrt{2}}\left(\frac{t-b}{2a}-\frac{a}{3c^2}\right)=\frac{\sqrt{3}}{2}\frac{(t-b)}{\sqrt{2}a}-\frac{a}{\sqrt{6}c^2}=\delta_x} \quad (112)$$

This concludes the discussion on the ingredients of the integrals (68) and (71).

---

[i] I am dedicating this journal paper to my Ph.D. Studies Academic Advisor Prof. John Orr. I wrote on my 2003 Ph.D. Dissertation: "On a more personal note, I am very grateful of Professor John A. Orr as a great example of an honest and just person, who lives in the "Fear of God," and who treats colleges equally and fairly. I would like to thank you, John, for your wisdom and courage, for believing in me and for being my academic advisor for the early part of my Ph.D. program." Prof. Orr was a phenomenal teacher, scholar, researcher, academic advisor, and Department Head.

[ii] A computation is any type of arithmetic or non-arithmetic calculation(s) that is well-defined; i.e., given the values of the parameters and of the main variable we can numerically determine the value of the main function or of the outcome. Common examples of computation are mathematical equation solving and the execution of computer algorithms. Mechanical or electronic devices (or, historically, people) that perform computations are known as calculators, computers. MATLAB is an example of a personal computer (PC) software that enables the computation of extremely difficult equations which cannot be solved my means of other calculators or other computers or other computer software. The word computation occurs very frequently in many of the publications of Giftet Journal of Geolocation, Geoinformation, and Geo-intelligence because it involves the computations of mathematical equations, integrals, or other mathematical algorithms that cannot be accurately and efficiently computed by means of other mathematical software.

[iii] KFT: Kummer's First Transformation.

[iv] The femto is a unit prefix in the International System of Units (SI) that represents a factor of 10^−15, or one quadrillionth. The prefix is derived from the Danish word femten, which means *fifteen*.

[v] Ditto iv.

[vi] Ditto Progri(2020, [6]) EN vii.